DOI: 10.1002/chem.200600139

Homo- and Heteropolynuclear Platinum Complexes Stabilized by Dimethylpyrazolato and Alkynyl Bridging Ligands: Synthesis, Structures, and Luminescence

Juan Forniés,*[a] Sara Fuertes,[a] Antonio Martín,[a] Violeta Sicilia,*[b] Elena Lalinde,*[c] and M. Teresa Moreno[c]

Dedicated to Professor V. Riera on the occasion of his 70th anniversary

Abstract: This work describes the synthesis of *cis*-[Pt(C≡CPh)$_2$(Hdmpz)$_2$] (**1**) and its use as a precursor for the preparation of homo- and heteropolynuclear complexes. Double deprotonation of compound **1** with readily available M^I (M = Cu, Ag, Au) or M^{II} (M = Pd, Pt) species affords the discrete hexanuclear clusters [{PtM$_2$(μ-C≡CPh)$_2$(μ-dmpz)$_2$}$_2$] [M = Cu (**2**), Ag (**3**), Au (**4**)], in which both "Pt(C≡CPh)$_2$-(dmpz)$_2$" fragments are connected by four d^{10} metal centers, and are stabilized by alkynyl and dimethylpyrazolate bridging ligands, or the trinuclear complexes [Pt(μ-C≡CPh)$_2$(μ-dmpz)$_2${M-(C^P)}$_2$] (M = Pd (**5**), Pt (**6**); C^P = CH$_2$-C$_6$H$_4$-P(*o*-tolyl)$_2$-κ*C*,*P*), respectively. The X-ray structures of complexes **1**–**4** and **6** are reported. The X-ray structure of the platinum–copper derivative **2** shows that all copper centers exhibit similar local geometry being linearly coordinated to a nitrogen atom and η^2 to one alkynyl fragment. However in the related platinum–silver (**3**) and platinum–gold (**4**) derivatives the silver and gold atoms present three different coordination environments. The complexes have been studied by absorption and emission spectroscopy. The hexanuclear complexes exhibit bright luminescence in the solid state and in fluid solution (except **4** in the solid state at 298 K). Dual long-lived emission is observed, being clearly resolved in low-temperature rigid media. The low-energy emission is ascribed to MLM′CT Pt(d)/π-(C≡CPh)→Pt(p_z)/M′(sp)/π*(C≡CPh) modified by metal–metal interactions whereas the high-energy emission is tentatively attributed to an emissive state derived from dimethylpyrazolate-to-metal (d^{10}) LM′CT transitions π-(dmpz)→M′(d^{10}).

Keywords: cluster compounds · heterometallic complexes · metal–metal interactions · N ligands · Pi interactions

[a] Prof. Dr. J. Forniés, S. Fuertes, Dr. A. Martín
Departamento de Química Inorgánica
Instituto de Ciencia de Materiales de Aragón
Facultad de Ciencias, Universidad de Zaragoza-CSIC
Plaza. S. Francisco s/n 50009 Zaragoza (Spain)
Fax: (+34) 976-761-159
E-mail: juan.fornies@unizar.es

[b] Dr. V. Sicilia
Departamento de Química Inorgánica
Instituto de Ciencia de Materiales de Aragón
Escuela Universitaria de Ingeniería Técnica Industrial, Universidad de Zaragoza-CSIC
Campus Universitario del Actur
Edificio Torres Quevedo, 50018 Zaragoza (Spain)
Fax: (+34) 976-762-189
E-mail: sicilia@unizar.es

[c] Dr. E. Lalinde, Dr. M. T. Moreno
Departamento de Química
Grupo de Síntesis Química de La Rioja, UA-CSIC
Universidad de La Rioja 26006 Logroño (Spain)
Fax: (+34) 941-299-621

Introduction

The chemistry of metal alkynyl complexes has long been investigated because of their rich chemical reactivity, structural diversity,[1–3] and more recently, due to their potential application in materials science.[4–21] In the chemistry of alkynyl platinum complexes increasing attention has been paid to the study of the spectroscopic and luminescence behavior of discrete polynuclear platinum complexes containing alkynyl bridging ligands because of their ability to modulate them by metal–metal (Pt···Pt, Pt···M) and η^2-metal alkynyl bonding interactions.[5,22–31]

Furthermore, polynuclear transition-metal complexes with neutral pyrazoles (HRpz) or anionic pyrazolates (Rpz) as ligands have attracted much attention due to their versatile structures and properties.[32–35] Pyrazolates such as 1,2-dihapto ligands have been used to produce numerous homo- and

heterobridged dinuclear complexes and oligomers. These kinds of ligands have a proven ability to hold metal atoms in close proximity while permitting a wide range of intermetallic separations, being useful in the synthesis of shape-persistent macrocycles, such as the homonuclear $[M^{I}(\mu\text{-Rpz})]_3$ (M = Cu,[36–42] Ag,[37,38,43,44] Au;[43,45–50] Rpz = pyrazolate or substituted pyrazolate) or $[M^{II}_3(\mu\text{-Rpz})_6]$ (M^{II} = Pd[51,52] Pt[52,53]) as the heteronuclear clusters $[Pd_2M_2(\mu\text{-Rpz})_6]$ (M = Cu, Ag, Au),[52,54] and $[M_2M'_4(\mu\text{-Rpz})_8]$ (M = Pd, Pt; M′ = Cu, Ag).[52,55] Apart from the interest arising from their structural diversity, some of these pyrazolate bridging complexes have also been shown to be excellent systems for examining metallophilic interactions[49,56–62] and as luminescent materials.[49,56–59,63–66] One of the synthetic strategies used to obtain the above-mentioned heteropolynuclear pyrazolate complexes is the replacement of the proton in coordinated pyrazoles by the metal ions: Cu^{I}, Ag^{I}, and Au^{I}. The self-assembly of the resulting units gives the heterometallic clusters.

Following our recent interest in alkynyl luminescent heteropolynuclear complexes,[25–31] we decided to explore the chemistry of new platinum complexes containing these two kinds of ligands: alkynyl and pyrazole, the reactivities of which, with different metal species, could afford heterometallic clusters. In this paper, we report the preparation of *cis*-$[Pt(C{\equiv}CPh)_2(Hdmpz)_2]$ (**1**), that can be easily deprotonated affording hexanuclear "Pt_2M_4" (M = Cu, Ag, Au) and trinuclear "PtM_2" (M = Pd, Pt) alkynyl dimethylpyrazolate bridging complexes. The structural characterization (compounds **1**–**4** and **6**) and luminescence behavior of the novel heteroleptic and heterometallic complexes is included.

Abstract in Spanish: *Este trabajo describe la síntesis de* cis-*[Pt(C≡CPh)$_2$(Hdmpz)$_2$] (**1**) y su empleo como precursor en la preparación de complejos homo- y heteropolinucleares. La doble desprotonación de **1** con especies de M^{I} (M = Cu, Ag, Au) y M^{II} (M = Pd, Pt) permite obtener clusters hexanucleares [{PtM$_2$(μ-C≡CPh)$_2$(μ-dmpz)$_2$}$_2$] [M = Cu (**2**), Ag (**3**), Au (**4**)], o complejos trinucleares [Pt(μ-C≡CPh)$_2$(μ-dmpz)$_2${M(C^P)}$_2$] (M = Pd (**5**), Pt (**6**); C^P = CH$_2$-C$_6$H$_4$-P(o-tolyl)$_2$-κC,P) respectivamente. En los complejos **2**–**4** ambos fragmentos "Pt(C≡CPh)$_2$(dmpz)$_2$" están conectados por cuatro centros metálicos de configuración d^{10}, estabilizados por ligandos alquinilo y/o dimetilpirazolato puente. Se describen las estructuras cristalinas de los complejos **1**–**4** y **6** obtenidas mediante difracción de rayos X sobre monocristales. La estructura cristalina del derivado de Pt/Cu, **2**, revela que todos los centros de cobre presentan una geometría local similar, y se encuentran coordinados linealmente a un átomo de nitrógeno y a un fragmento alquinilo de forma η^2. Sin embargo, en los derivados de Pt/Ag (**3**) y de Pt/Au (**4**) los átomos de plata y oro presentan tres entornos de coordinación diferentes. Se analizan los espectros de UV y de luminiscencia. Los compuestos hexanucleares presentan una intensa luminiscencia tanto en estado sólido como en disolución (excepto **4** en estado sólido a 298 K). Estos derivados exhiben una doble emisión de larga vida media, que se resuelve claramente en un medio rígido a baja temperatura. La emisión de baja energía se asocia a la transferencia de carga metal-ligando-metal′ MLM′CT Pt(d)/π(C≡CPh)→Pt(p$_z$)/M′(sp)/π*(C≡CPh) modificada por interacciones metal–metal mientras que la emisión de alta energía se atribuye a un estado emisivo derivado de transiciones desde el ligando dimetilpirazolato al metal′ (d^{10}) LM′CT π(dmpz)→M′(d^{10}).*

Results and Discussion

Synthesis and characterization of *cis*-[Pt(C≡CPh)$_2$(Hdmpz)$_2$] (1): Complex **1** was prepared in moderate yield (50%) by reaction of *cis*-$[PtCl_2(Hdmpz)_2]$ (**A**) with LiC≡CPh (see Scheme 1a and Experimental Section for details), and was characterized by the usual analytical and spectroscopic means, and also by X-ray crystallography. The IR spectrum of complex **1** shows several absorptions around 3200 cm^{-1} due to the N–H bonds and two $\tilde{\nu}$(C≡C) absorptions consistent with a *cis* configuration of the σ-alkynyl ligands around the Pt^{II} center.[67] The ^{1}H NMR spectrum shows, in addition to the aromatic Ph protons, two sets of signals due to the Hdmpz groups, indicating that they are inequivalent at room temperature, probably due to the hindered rotation around the Pt–N bonds. Variable-temperature ^{1}H NMR spectra of complex **1** revealed the coalescence of each pair of signals (δ = 1.37 and 1.87 (Me) at 320 K; 2.05 and 2.70 (Me) at 325 K; 5.65 and 5.86 (H^4) at 310 K; 11.71 and 12.99 ppm (N–H) at 330 K) and at 330 K only one set of dmpz signals (δ = 12.40 (N–H), 5.64 (H^4), 2.40, 1.64 ppm (CH$_3$)) is observed. An estimation of the energy barrier by using the approximation to the Eyring equation ($\Delta G^{\neq} = 19.14\,T_c(9.97+\log T_c/\Delta\nu)$) at the coalescence temperatures T_c leads to $\Delta G^{\neq}$ values of about 63 kJ mol^{-1} for the Pt–N bond rotation.

The structure of complex **1** as evaluated by X-ray diffraction analysis (Figure 1, Table 1) confirms the *cis* arrangement of both phenylethynyl and Hdmpz groups. The Pt–C bond lengths are identical within experimental error and similar to those reported for neutral diimine bis(alkynyl)platinum(II) complexes[68–70] but slightly shorter than those observed in other platinum alkynyl complexes such as $(NBu_4)[Pt(bzq)(C{\equiv}CPh)_2]$,[67] $(NBu_4)[Pt(bzq)(C{\equiv}C\text{-}C_5H_4N\text{-}2)_2]$,[67] $[Pt(t\text{Bu}_3\text{tpy})(C{\equiv}C\text{-}C_6H_4\text{-NCS-}4)](OTf)$,[71] and $[Pt(C{\equiv}CR)(Me_2NCH_2\text{-}(\sigma Fc))(dmso)]$ (R = $SiMe_3$ (2.076(5), Fc (2.059(6) Å).[72] The Pt–N bond lengths are in the range of those found in Pt complexes with the same type of ligands.[52,53,73–78] The platinum alkynyl units [Pt-C$_\alpha$≡C$_\beta$-C$_{Ph}$] basically show a linear arrangement with the C$_\alpha$ and C$_\beta$ bond angles ranging between 175 and 180°. The monodentate Hdmpz ligands are planar within experimental error and they are oriented almost perpendicularly one to another (the interplanar angle being 75.95°) forming, with the platinum coordination plane, an angle of 61.13° (N(1), N(2), C(17), C(18), C(19)) and 65.84° (N(3), N(4), C(22), C(23), C(24)).

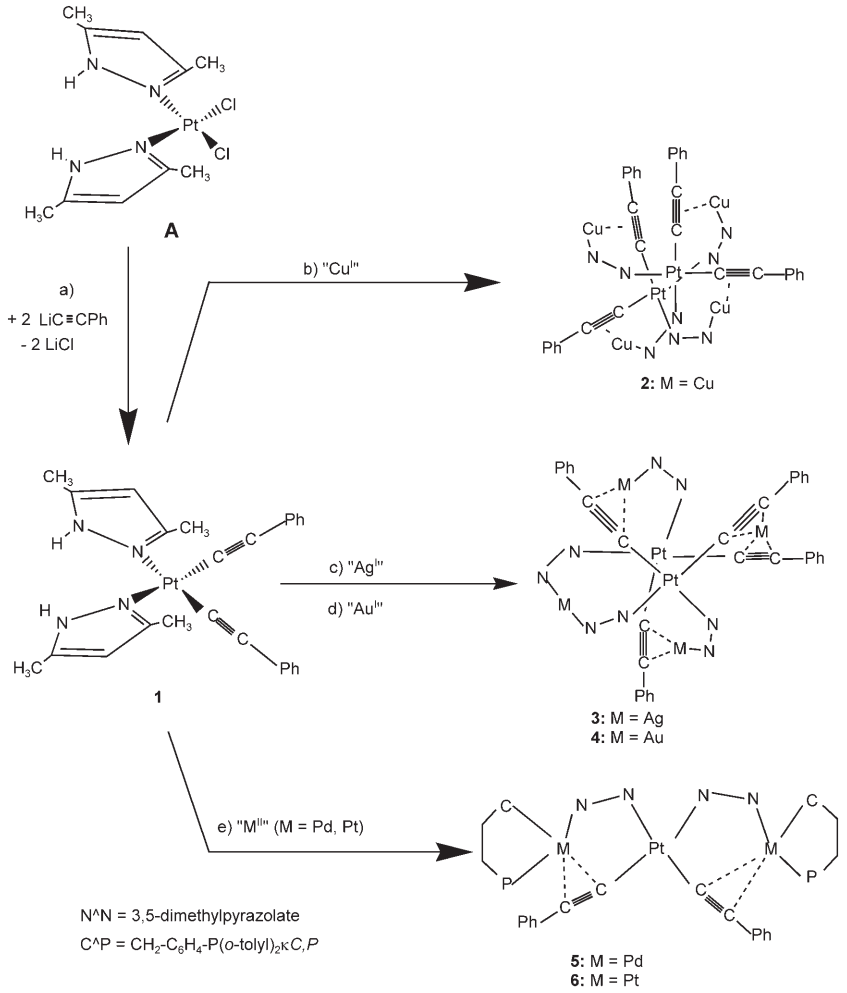

Scheme 1. b) $2[Cu(NCMe)_4]PF_6/NEt_3$ $(-2NEt_3HPF_6)$; c) $+2AgClO_4/NEt_3/(-2NEt_3HClO_4)$; d) 2PPN[Au(acac)$_2$]/$NEt_3$/(−2PPNacac/−2$NEt_3$Hacac); e) $[M(C\hat{}P)(\mu\text{-}O_2CCH_3)]_2)/NEt_3/(-2NEt_3HO_2CCH_3)$.

replaced by metal ions as Cu^I, Ag^I, and Au^I. The reactions of complex **1** with $[Cu(CH_3CN)_4]PF_6$, $AgClO_4$, and PPN[Au(acac)$_2$] (PPN = $Ph_2P{=}N^+{=}PPh_3$) in a 1:2 molar ratio in CH_2Cl_2 and, in the presence of NEt_3, thus result in the formation of the hexanuclear compounds $[\{PtM_2(\mu\text{-}C{\equiv}CPh)_2(\mu\text{-}dmpz)_2\}_2]$ (M = Cu (**2**), Ag (**3**), Au (**4**)) (Scheme 1b–d). In all cases the acidic protons are eliminated with formation of the corresponding triethylammonium salts (NEt_3HPF_6, NEt_3HClO_4, NEt_3Hacac), that are separated from the final complexes **2–4** due to their solubility in methanol that was used as a precipitating agent (see Experimental Section). The desired final complexes are isolated as air-stable yellow (**2**, **3**) or beige (**4**) solids and have been characterized by elemental analysis, mass spectrometry (FAB^+), IR and ^1H NMR spectroscopy, and also by single-crystal X-ray diffraction analysis. The most significant structural features are found in the IR spectra of the complexes. Thus, the absence of absorptions due to the N–H bonds and the significant shifts of the $\tilde{\nu}$(C≡C) stretching vibrations to lower wavenumbers with respect to those of the starting compound **1** (2127, 2115 (**1**) versus 2023, 1984 (**2**); 2039 (**3**); 1948 cm^{-1} (**4**)) indicate that in all cases the substitution of the acidic hydrogen atoms (N–H) by Cu^I, Ag^I, and Au^I atoms has taken place and that these metal atoms are presumably interacting with the electron density of the alkynyl ligands.[79–81] The FAB^+ mass spectra of all complexes exhibit a high-intensity peak corresponding to $[Pt_2M_4(C{\equiv}CPh)_4(dmpz)_4]$ in agreement with a dimeric formulation that has been confirmed by X-ray crystallography (Figures 2–4).

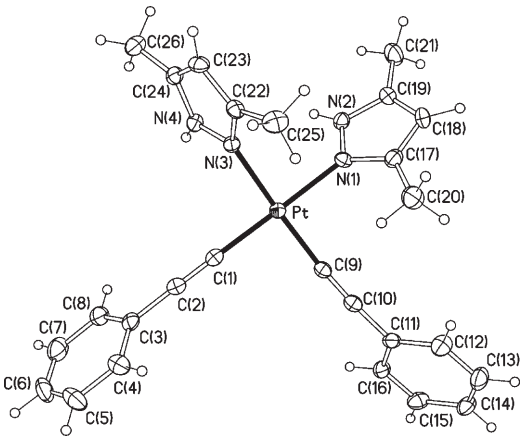

Figure 1. Molecular structure of compound **1** (ellipsoids at 50% probability).

Table 1. Selected bond lengths [Å] and angles [°] in complex *cis*-[Pt(C≡CPh)$_2$(Hdmpz)$_2$] (**1**).

Pt–C(1)	1.957(3)	C(9)–C(10)	1.201(4)
Pt–N(1)	2.074(3)	Pt–C(9)	1.951(3)
C(1)–C(2)	1.196(4)	Pt–N(3)	2.066(3)
Pt-C(1)-C(2)	177.0(3)	C(1)-C(2)-C(3)	179.1(4)
Pt-C(9)-C(10)	175.3(3)	C(9)-C(10)-C(11)	176.2(3)

Reactivity of *cis*-[Pt(C≡CPh)$_2$(Hdmpz)$_2$] (1) towards M^I species (M = Cu, Ag, Au): The two acidic hydrogen atoms in complex **1** can be eliminated by a weak Lewis base and

Structural characterization of complexes 2–4: Complex **2** (Figure 2, Table 2) is a hexanuclear compound formed by two $Pt(C{\equiv}CPh)_2(dmpz)_2$ fragments held together by four copper atoms, each σ-bonded to one dmpz from one platinum unit and η^2-bonded to the phenylethynyl ligand from the other one. The platinum coordination planes are almost parallel (interplanar angle 9.5(1)°)[82] and staggered with a torsion angle N(3)-Pt(1)-Pt(2)-N(7) of 31.5° appropriate to a local η^2 and σ (N, dmpz) dicoordination of the Cu centers. All Cu atoms adopt a linear coordination with similar geometric environments, formed by the N atom and the midpoint of the coordinated C≡C vector (C_0), as the N-Cu-C_0 angles are 169.2° (Cu(1)), 171.9° (Cu(2)), 171.9° (Cu(3)), and 171.9° (Cu(4)). The C≡CPh ligands are nearly symmetrically η^2-coordinated to the Cu^I centers with Cu–C bond lengths that are comparable to those found in related Cu^I π-bonded alkynyl bridging complexes.[25,83–91] As far as we know, a small number of Cu^I complexes with an L-Cu(η^2-C≡CR) coordination environment have been reported.[83–85] The Cu–N and Pt–N bond lengths are in the range of those found in pyrazolato copper(I)[36–42,56,57,63,92] and Pt^{II} complexes.[52,53,73–78] As expected[79–81] the Pt-$C_\alpha{\equiv}C_\beta$-C_{Ph} units deviate from linearity, this distortion being more pronounced at the C_β atom (161.7(6)–167.5(7)°) and the $C_\alpha{\equiv}C_\beta$ bond lengths are slightly elongated with respect to complex **1**.

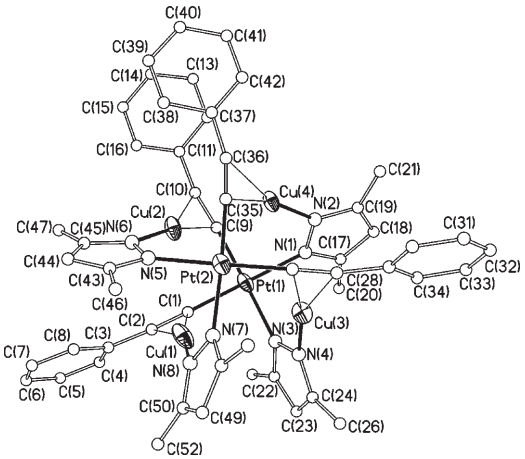

Figure 2. Molecular structure of compound **2** (ellipsoids at 50% probability).

Finally, no bonding between the metal atoms occurs (Pt···Cu 3.016(9)–3.348(9) Å; Cu···Cu 3.089(9)–4.695(2) Å). Although, we noted that the two shortest Pt···Cu contacts are associated with the alkynyl bridging fragments (3.016–3.121 versus 3.224–3.348 Å). With regard to the Cu···Cu distances, although the Cu(1)···Cu(2) and Cu(2)···Cu(4) (3.236(4) and 3.089(9) Å, respectively) are longer than the sum of van der Waals radii (2.8 Å),[93] both are short enough for a contact between the atoms to be considered.

The molecular structures of complexes **3** and **4** are depicted in Figures 3 and 4 and selected bond lengths and angles are listed in Table 3. As can be seen, both hexanuclear complexes are formed by two "$Pt(C{\equiv}CPh)_2(dmpz)_2$" fragments joined by four M^I atoms (M = Ag (**3**), Au (**4**)), in such a way that the platinum coordination planes are again almost parallel (the interplanar angle is 8.5° in complex **3** and 9.3° in complex **4**).[82] However, in these complexes, the torsion angle N(1)-Pt-Pt′-N(1′) is 53.0° in complex **3** and 45.9° in complex **4**, respectively, allowing the metal centers (Ag in complex **3** and Au in complex **4**) to exist in different local environments. Thus, each of the four M atoms is bonded to two ligands, one from each platinum unit (Pt, Pt′) but exhibits three different coordination environments: M(1) is symmetrically stabilized by the electron density of two alkynyl ligands, M(2) is coordinated to two dmpz groups, while both M(3) and M(3′) are bonded to one dmpz and to the π electron density of one alkynyl ligand. All the M atoms can be considered to have a linear coordination environment; for M(1), the angles C_0-M(1)-C_{00} (C_0 and C_{00} being the midpoints of the two C≡C vectors coordinated to it) are 157.8° (**3**) and 174.5° (**4**), for M(2), the angles N(2)-M(2)-N(2′) are 168.3(2)° (**3**) and 173.2(3)° (**4**), and for M(3) and M(3′) the angles N-M-C_0 are 166.2° (**3**) and 175.3° (**4**), respectively. With the exception of the asymmetrical η^2,η^2-coordination for Ag(1) in complex **3**, the remaining C≡CPh ligands are essentially coordinated in a symmetrical η^2-coordination mode to the M centers, with similar M–C_α and M–C_β lengths and comparable to those observed in other dicoordinated η^2-alkynyl-bonded Ag^I[79,86,94–99] or Au^I[100–104] complexes. The structural details concerning the C≡CPh units are typical of μ,η^2 (σ,π) alkynyl bridging complexes.[79–81] In particular, the Pt-$C_\alpha{\equiv}C_\beta$-C_{Ph} units are not strictly linear (see Table 3) and the $C_\alpha{\equiv}C_\beta$ bond lengths are comparatively longer than for typical terminal alkynyl complexes. It is interesting to note that these C≡C distances are somewhat more elongated in the platinum–gold derivative (**4**) (average 0.052 Å in complex **4** versus 0.03 Å in complex **3**) with re-

Table 2. Selected bond lengths [Å] and angles [°] in complex [{$PtCu_2$(μ-C≡CPh)$_2$(μ-dmpz)$_2$}$_2$] (**2**).

Pt(1)–N(1)	2.051(4)	Pt(1)–N(3)	2.013(6)
Pt(2)–C(27)	1.961(6)	Pt(2)–C(35)	1.895(8)
Pt(2)–N(5)	2.054(5)	Pt(2)–N(7)	2.025(6)
Cu(1)–C(1)	2.010(7)	Cu(1)–C(2)	2.063(6)
Cu(1)–N(8)	1.881(6)	Cu(2)–C(9)	2.004(4)
Cu(2)–C(10)	2.097(6)	Cu(2)–N(6)	1.882(4)
Cu(3)–C(27)	2.018(6)	Cu(3)–C(28)	2.067(6)
Cu(3)–N(4)	1.873(5)	Cu(4)–C(35)	2.012(6)
Cu(4)–C(36)	2.072(6)	Cu(4)–N(2)	1.867(4)
C(1)–C(2)	1.217(7)	C(9)–C(10)	1.267(9)
C(27)–C(28)	1.235(8)	C(35)–C(36)	1.258(9)
Pt(1)–Cu(1)	3.121(8)	Pt(1)–Cu(2)	3.016(9)
Pt(1)–Cu(3)	3.274(8)	Pt(1)–Cu(4)	3.283(7)
Pt(2)–Cu(1)	3.224(8)	Pt(2)–Cu(2)	3.348(9)
Pt(2)–Cu(3)	3.048(7)	Pt(2)–Cu(4)	3.078(7)
Cu(1)–Cu(2)	3.236(4)	Cu(2)–Cu(4)	3.089(9)
Cu(1)···Cu(3)	3.585(1)	Cu(1)···Cu(4)	4.683(1)
Cu(2)···Cu(3)	4.695(2)	Cu(3)···Cu(4)	3.379(1)
Pt(1)-C(1)-C(2)	177.3(5)	C(1)-C(2)-C(3)	167.5(7)
Pt(1)-C(9)-C(10)	176.0(5)	C(9)-C(10)-C(11)	165.8(6)
Pt(2)-C(27)-C(28)	173.6(5)	C(27)-C(28)-C(29)	164.6(7)
Pt(2)-C(35)-C(36)	174.2(5)	C(35)-C(36)-C(37)	161.7(6)

spect to those in complex **1**. This fact concerning the structure, that is in line with the lower (C≡C) vibration observed in the IR spectra ($\tilde{\nu}$ = 1948 in complex **4** as opposed to 2039 cm^{-1} in complex **3**), clearly points to a stronger Au-η^2 (acetylenic) bonding interaction, contrasting with the relatively low number of reported complexes of type bis(η^2-alkynyl)Au.[103] The Pt–C,[67–72,79–81] Pt–N,[52,53,73–78] and M–N bond lengths[37,38,43–50,52,54,55,64,92,105–111] are similar to those observed in related pyrazolate complexes.

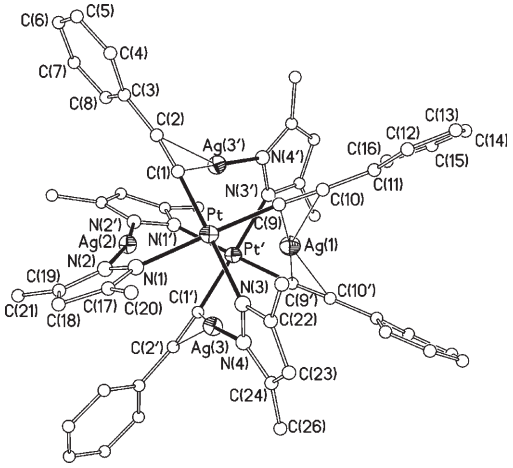

Figure 3. Molecular structure of compound **3** (ellipsoids at 50% probability).

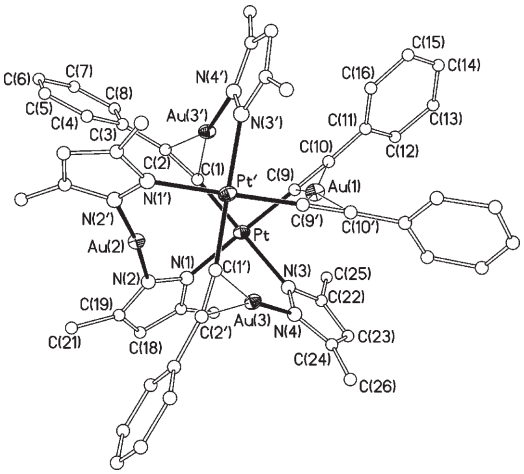

Figure 4. Molecular structure of compound **4** (ellipsoids at 50% probability).

Although the M···M separations are all longer than 3 Å (3.027(5)–4.473(6) (**3**); 3.297(3)–5.010(5) Å (**4**)), some metal–metal (Pt···M and also M···M) contacts could be invoked. In both complexes, the shortest Pt···M length is that corresponding to the M(1) atom, established by η^2,η^2 alkynyl ligands (3.094(4) and 3.297(3) Å for complexes **3** and **4**, respectively). Among the M···M distances, only the M(1)···M(2) is long enough to exclude any bonding contact between the metal atoms (4.473(6) and 5.010(5) Å for complexes **3** and **4**, respectively) though, in general, the Ag···Ag separations (3.027(5), 3.280(5) Å) are shorter than those for the Au···Au separations (3.411(4), 3.573(3) Å).

Table 3. Selected bond lengths [Å] and angles [deg] for [{PtM_2(μ-C≡CPh)$_2$(μ-dmpz)$_2$}$_2$]·2Me_2CO.

	M = Ag (**3**·2Me_2CO)	M = Au (**4**·2Me_2CO)
Pt–C(1)	1.969(4)	1.967(6)
Pt–C(9)	1.971(5)	1.949(7)
Pt–N(1)	2.061(4)	2.067(5)
Pt–N(3)	2.066(4)	2.065(5)
M(1)–C(9)/(9′)	2.289(4)	2.217(6)
M(1)–C(10)/(10′)	2.434(5)	2.225(7)
M(2)–N(2)/(2′)	2.081(3)	2.025(5)
M(3)–N(4)	2.102(3)	2.030(5)
M(3)–C(1′)	2.276(4)	2.221(6)
M(3)–C(2′)	2.323(4)	2.174(6)
Pt–M(1)	3.094(4)	3.297(3)
Pt–M(2)	3.589(4)	3.670(3)
Pt–M(3)	3.314(4)	3.471(4)
M(1)–M(2)	4.473(6)	5.010(5)
M(1)–M(3)	3.027(5)	3.411(4)
M(2)–M(3)	3.280(5)	3.573(3)
C(1)–C(2)	1.233(6)	1.246(9)
C(9)–C(10)	1.224(7)	1.255(10)
N(2′)-M(2)-N(2)	168.3(2)	173.2(3)
C(2)-C(1)-Pt	176.1(4)	172.8(5)
C(1)-C(2)-C(3)	168.5(4)	164.0(6)
C(10)-C(9)-Pt	174.2(4)	178.0(6)
C(9)-C(10)-C(11)	174.4(5)	159.1(8)

Behavior of compounds 2–4 in solution: The IR spectra of all solutions of complexes in CH_2Cl_2 show similar $\tilde{\nu}$(C≡C) absorptions to those in the solid state, suggesting that the η^2-alkynyl interactions probably remain when in solution. For the ^{1}H NMR spectra of these complexes, in the light of the structures of complexes **2**–**4** as determined by X-ray diffraction (Figures 2–4), two sets of signals, due to the inequivalent dmpz groups of one Pt(C≡CPh)$_2$(dmpz)$_2$ unit, are expected. This is, in fact, what it is observed for complexes **2** and **4** (symmetry C_2). However, complex **3** shows only one set of signals due to the dmpz groups (δ = 5.85 (s, H^4), 2.29 (s, CH_3), 1.90 ppm (s, CH_3)), indicating that either the complex exhibits a structure of higher symmetry in solution (Scheme 2c, C_{2h}) or that some dynamic process takes place on the NMR time scale. Low-temperature NMR experiments in solutions of CD_2Cl_2 were carried out. At 243 K the singlet at 2.29 ppm becomes wider and splits into two singlets at 228 K (δ = 2.42 (s), 2.00 ppm (s)), but the other signals do not change. At 203 K all signals split, giving rise to two different sets of resonances due to the dmpz (δ = 5.91 (s, 1H; H^4), 5.86 (s, 1H; H^4), 2.40 (s, 3H; CH_3), 2.00 (s, 3H; CH_3), 1.94 (s, 3H; CH_3), 1.81 ppm (s, 3H; CH_3)). Successive experiments on the same sample at 193 and 273 K show two and one sets of signals for the dmpz, respectively, indicating the existence of a reversible process. The behavior of complex **3** in solution could be related to the fact that the η^2-alkynyl Ag bonding interactions are relatively weaker than the corresponding η^2-alkynyl metal bonding interactions in

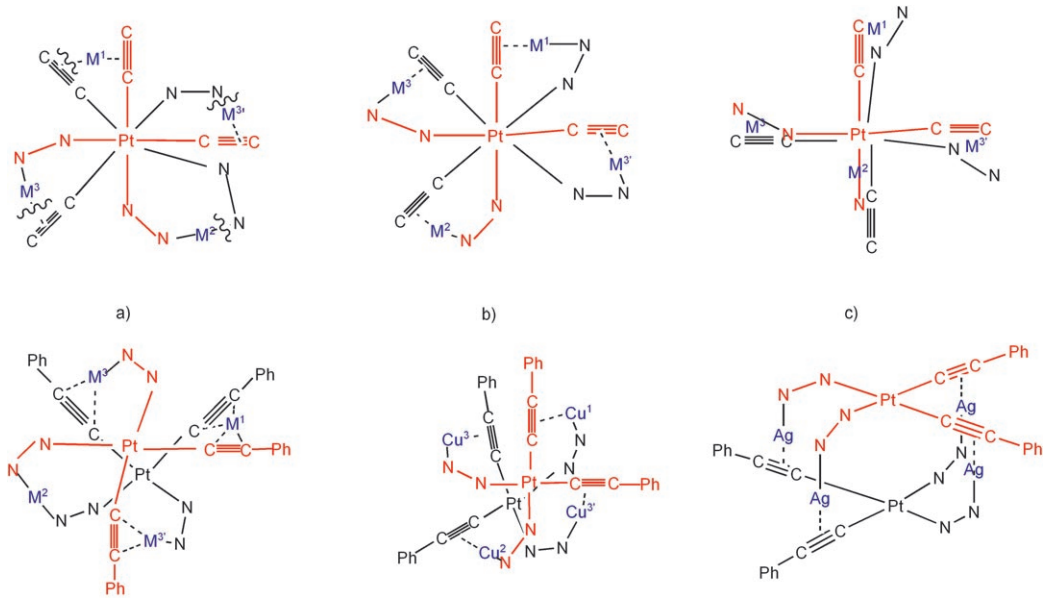

Scheme 2. a) Solid-state structure for M = Ag, Au; b) solid-state structure for M = Cu; c) proposed structure for complex **3** in solution at room temperature.

the homologous copper (**2**) and gold (**4**) derivatives and, at room temperature, complex **3** (structure a) reaches the structure c through the intermediate structure b. As is shown in Scheme 2, structure b, found in the copper derivative, can be easily obtained from structure a through intramolecular-ligand-site exchange by the simultaneous cleavage of two η^2 interactions (Ag(1), Ag(3)), and two silver–dmpz bonds (Ag(3′) and Ag(2)). Subsequent or simultaneous rotation of one of the platinum fragments (~45°) could give rise to the most symmetrical structure c. This suggestion is supported by the fact that the NMR spectrum of complex **4** does not change with increasing the temperature from 293 to 323 K, while the proton spectrum of complex **2** at high temperature (320 K) shows the same pattern ($\delta = 5.73$ (s, 2H; H^4), 2.45 (s, 3H; CH_3), 2.00 (s, 3H; CH_3), 1.78 ppm (s, 6H; CH_3)), as that of complex **3** at room temperature (293 K). This fact suggests that, in solution, these structures a, b, and c are probably related, and the rigidity increases (**3** < **2** < **4**) as the $\tilde{\nu}$(C≡C) in solution decreases ($\tilde{\nu}$ = 2043 (**3**); 2026, 1989 (**2**); 1959 cm^{-1} (**4**)). In fact, although complex **3** adopts structure a in the solid state, we cannot exclude that the frozen structure present in the low-temperature regime (228 K) may correspond to a b-type structure, since a similar pattern (inequivalent dmpz groups) should be observed.

Reactivity of *cis*-[Pt(C_2Ph)$_2$(Hdmpz)$_2$] (1) towards the [{M(C^P)(μ-O_2CCH_3)}$_2$] species (M = Pd, Pt; C^P = CH_2-C_6H_4-P(*o*-tolyl)$_2$-κ*C*,*P*): Complex **1** also reacts with the dinuclear neutral complexes [{M(C^P)(μ-O_2CCH_3)}$_2$] (M = Pd, Pt; C^P = CH_2-C_6H_4-P(*o*-tolyl)$_2$-κ*C*,*P*) in a 1:1 molar ratio in the presence of NEt_3 to yield the trinuclear complexes [Pt(μ-C≡CPh)$_2$(μ-dmpz)$_2${M(C^P)}$_2$] (M = Pd (**5**), Pt (**6**)) in high yield (Scheme 1e). The ammonium salt (NEt_3-HO_2CCH_3) can be eliminated because it is soluble in methanol, used as the precipitating agent for complexes **5** and **6** (see Experimental Section). Both derivatives are stable in air and moisture and have been characterized by common analytical and spectroscopic methods. The structure of complex **6** has been also confirmed by X-ray crystallography. The IR spectra of compounds **5** and **6** confirm the substitution of the acidic hydrogen atoms (N–H) by Pd^{II} or Pt^{II} species, since no absorptions due to the N–H bonds are observed and the η^2-coordination of these metal centers to the alkynyl ligands,[79–81] because the $\tilde{\nu}$(C≡C) absorptions, appear significantly shifted to lower wavenumbers in relation to the precursor (see Experimental Section).

The X-ray study on complex **6** shows (Figure 5, Table 4) it to be a trinuclear species of Pt^{II}, in which the central Pt(C≡CPh)$_2$(dmpz)$_2$ unit is joined to two Pt(C^P) fragments by a hetero-bridged system formed by a dmpz and a μ,η^2-phenylethynide ligand. In the central Pt(C≡CPh)$_2$(dmpz)$_2$ unit, the

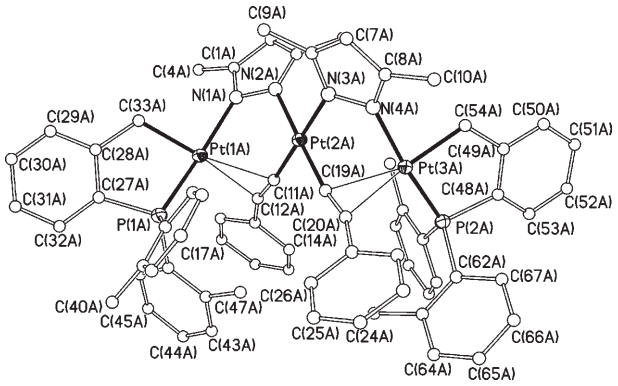

Figure 5. Molecular structure of compound **6** (ellipsoids at 50% probability).

Table 4. Selected bond lengths [Å] and angles [°] in complex [Pt(μ-C≡CPh)$_2$(μ-dmpz)$_2${Pt(C^P)}$_2$] **6**·CH_2Cl_2.

Pt(1)−C(33)	2.066(7)	C(19)−C(20)	1.236(8)
Pt(1)−P(1)	2.209(2)	Pt(1)−N(1)	2.089(5)
Pt(1)−C(12)	2.308(6)	Pt(1)−C(11)	2.278(6)
Pt(2)−N(3)	2.066(5)	Pt(2)−N(2)	2.054(5)
Pt(3)−C(54)	2.058(6)	Pt(3)−P(2)	2.224(2)
Pt(3)−N(4)	2.085(5)	Pt(3)−C(20)	2.324(6)
Pt(3)−C(19)	2.297(6)	Pt(2)−Pt(3)	3.213(5)
C(11)−C(12)	1.226(8)	Pt(1)−Pt(2)	3.256(1)
Pt(2)-C(11)-C(12)	171.0(5)	C(11)-C(12)-C(13)	160.8(7)
Pt(2)-C(19)-C(20)	167.8(5)	C(19)-C(20)-C(21)	159.8(6)

platinum atom exhibits a slightly distorted square-planar coordination environment, with the angles between *cis* ligands deviated from the theoretical value. The Pt(2)−N and central Pt−C σ bond lengths are in the range of those found in related pyrazolate[52,53,73–78] and μ,η^2-alkynyl platinum(II) complexes,[67–72,79–81] and the structural details concerning the alkynyl fragments are common for μ,η^2-alkynyl ligands.[79–81]

The side platinum atoms, Pt(1A) and Pt(3A), exhibit a distorted square-planar environment that is considered to be formed by the C and P donor atoms of the cyclometalated phosphine, the N atom of the bridging dmpz and the midpoint ((X(1A) for Pt(1A), X(1B) for Pt(3A)) of the π-bonded $C_\alpha{\equiv}C_\beta$ vector; the angles between *cis* ligands deviate significantly from 90°. The platinum alkynide η^2 linkages are almost symmetrical with the Pt−C_α distances only slightly shorter than the corresponding Pt−C_β ones. All bond lengths around Pt(1A) and Pt(3A) are in the range of those found for C^P,[78,112–115] pyrazolate,[52,53,73–78] and η^2-alkynyl platinum(II) complexes.[81,116–119] The terminal platinum coordination planes are almost perpendicular to that of the central platinum Pt(2A) plane, the dihedral angles being 79.8° for Pt(1A) and 82.9° for Pt(3A); the dihedral angle between both terminal coordination planes is 27.9°.

In solution, both complexes **5** and **6** show the expected signals corresponding to one half of the molecule, in agreement with the molecular structure observed for complex **6** (see Experimental Section).

Absorption and emission spectroscopy on complexes 1–6: The absorption and emission spectra and other photophysical data are summarized in Tables 5 and 6. In CH_2Cl_2 solution, the absorption spectrum of the mononuclear alkynyl complex **1** displays intense high-energy bands (220–274 nm) and a relatively weak shoulder at 315 nm ($\varepsilon = 8600\,M^{-1}cm^{-1}$). The very high-energy bands at 220 (sh), 230 nm ($32\,200\,M^{-1}cm^{-1}$) that are also present in the bischloride precursor *cis*-[$PtCl_2$(Hdmpz)$_2$] (220 (sh), 235 nm), are assigned as intraligand π→π* transitions of Hdmpz, while the structured band with maxima at 267 and 274 nm, that are absent in the precursor, seems to correspond to π→π* transitions in the C≡CPh ligands. On the basis of previous assignments[5,10,120–124] and theoretical studies,[120,125–127] the low-energy shoulder that is observed at 315 nm in CH_2Cl_2 and slightly blue-shifted in NCMe (310 nm), is attributed tentatively to an admixture of π→π*(C≡CPh) IL/dπ(Pt)→π*(C≡CPh) MLCT.[128] In agreement with this assignment, the band is notably blue-shifted in relation to that seen in the homoleptic derivative (NBu_4)$_2$[Pt(C≡CPh)$_4$] (347 nm)[127] in which its dianionic nature presumably increases the energy of the HOMO (dπ(Pt)/π(C≡C)),[128] decreasing the energy of the corresponding ^{1}MLCT transition. By comparison, a band at 328 nm in complex *trans*-[$Pt(PEt_3)_2$(C≡CPh)$_2$] has been also assigned to the ^{1}MLCT transition Pt(5d)→(C≡CPh),[129] though on the basis of recent theoretical calculations on *trans*-[$Pt(PH_3)_2$(C≡CPh)$_2$] as a model, the low-energy absorption has been reassigned as intraligand in nature (HOMO 25% d_{xz}(Pt), 75% C≡CAr and LUMO 20% p_x(Pt), 41% PH_3 and 39% C≡CAr).[130]

Table 5. Absorption data for complexes **A**, **1**–**6** (CH_2Cl_2 ~ 5×10^{-5} M solutions).

Compound	Absorption ($10^3\,\varepsilon$ $M^{-1}\,cm^{-1}$)
A	220 sh (11.9), 235 (27.3)
1	220 sh (12.8), 230 (32.2), 261 (28.4), 267 (33.2), 274 (34.6), 315 sh (8.6)
	225 (34.9), 235 (32.5), 266 (36.2), 273 (38.3), 298 sh (22.1), 310 (9) (NCMe)
2	222 sh (13.0), 240 (58.8), 267 (46.8), 273 (49.7), 346 br (16.9)
3	222 sh (14.0), 237 (54.8), 267 (43.6), 273 (44.7), 331 br (17.7)
4	216 sh (13.9), 245 (51.9), 290 (30.2), 330 br (12.4)
5	236 (45.9), 281 (35.3), 318[a] (23.1)
6	236 (48.6), 281 (63.9), 332[a] (41.1)

[a] With a tail to 410–420 nm.

The absorption spectra of the hexanuclear Pt_2M_4 complexes **2**–**4** (Figure 6) show the expected high-energy intraligand bands and are characterized by a low-energy band that appears at 346 nm in the platinum–copper complex **2**, and is slightly blue-shifted in the platinum–silver **3** (331 nm) and the platinum–gold **4** (330 nm) derivatives. We attributed this to the [Pt_2M_4(C≡CPh)$_4$] core, being mainly associated with the IL/MLCT (Pt→C≡CPh) transition, probably mixed with metal (d^{10}) orbitals. Clearly, the mixed IL (π→π*(C≡CPh))/MLCT (dπ(Pt)→π*(C≡CPh)) transition in the precursor **1** (315 nm) should be red-shifted by the increased π-accepting ability of the phenylethynyl groups upon η^2-coordination to the d^{10} metal centers.[5,131–134] Therefore, the low-energy absorption is tentatively assigned as an admixture of MLCT (Pt/π(C≡CPh)→π*(C≡CPh)) and LM′CT (ligand- or platina-ligand-M′ charge transfer Pt-C≡CPh→M′(d^{10})) probably modified by additional Pt···M′(d^{10}) metal–metal interactions. Alternatively, the transition may be viewed as an MLM′CT (M = Pt, M′ = d^{10}) with intraligand alkynyl character. This assignment is similar to those previously made in related heteropolymetal η^2-alkynyl bridging complexes (σ-Pt, η^2···M)[132,133,135,136] though, as stated by Yam and co-workers,[136] in this type of system one should be aware that assignments of electronic transitions between metal and/or ligand localized orbitals are only rough approximations due to possible orbital mixing. In complexes **3** and **4** some contribution of ligand (dmpz)-to-M′(d^{10}) LM′CT cannot be ex-

Table 6. Photophysical data for complexes **1**–**4**.

Compound	Medium (T [K])	λ_{max}^{em} [nm]	τ [μs]	Φ[a]
cis-[Pt(C≡CPh)$_2$(Hdmpz)$_2$] (**1**)	solid (298)	[b]		
	solid (77)	432 max (with tail to 600) (λ_{ex} 300–360)	44(432) λ_{ex} 320	
	CH_2Cl_2 10^{-3} M (298)	[b]		
	CH_2Cl_2 10^{-3} M (77)	427 max, 450, 465 (λ_{ex} 300–320)		
[{PtCu$_2$(μ-C≡CPh)$_2$(μ-dmpz)$_2$}$_2$] (**2**)	solid (298)	570 (λ_{ex} 350–400)		
		565 sh, 580 max (λ_{ex} 420)	27(545), 29(580) λ_{ex} 420	
	solid (77)	570 (λ_{ex} 350–370)		
		570 max, 650 sh (λ_{ex} 400)	92(570), 69(650) λ_{ex} 400	
	CH_2Cl_2 10^{-3} M (298)	640–660 (λ_{ex} 400–420)		2.82×10^{-3}
	CH_2Cl_2 10^{-3} M (77)	590 (λ_{ex} 380)		
		570 sh, 635 (λ_{ex} 410)		
[{PtAg$_2$(μ-C≡CPh)$_2$(μ-dmpz)$_2$}$_2$] (**3**)	solid (298)	560 (λ_{ex} 420)	10(560) λ_{ex} 420	
		480 sh, 550 max (λ_{ex} 330–380)		
	solid (77)	480 max, 570 (λ_{ex} 320–370)	17(480), 16(570) λ_{ex} 370	
		480 min, 570 (λ_{ex} 420)		
		570 (λ_{ex} 450)	15(570) λ_{ex} 450	
	CH_2Cl_2 10^{-3} M (298)	487 min, 570 max (λ_{ex} 360–380)		2.50×10^{-2}
		570 (λ_{ex} 420)		
	CH_2Cl_2 10^{-3} M (77)	470 (λ_{ex} 320)		
		470 max, 580 min (λ_{ex} 370)		
		470, 580 (λ_{ex} 400)		
		470 min, 585 max (λ_{ex} 420)		
		585 (λ_{ex} 430–460)		
[{PtAu$_2$(μ-C≡CPh)$_2$(μ-dmpz)$_2$}$_2$] (**4**)	solid (298)	[b]		
	solid (77)	590 (λ_{ex} 360–420)	16(590) λ_{ex} 380	
	CH_2Cl_2 10^{-3} M (298)	622 (λ_{ex} 370–400)		1.58×10^{-3}
	CH_2Cl_2 10^{-3} M (77)	446, 475 sh, 575 (λ_{ex} 380)		
		446, 475 sh, 560, 610 sh (λ_{ex} 400)		

[a] Measured by using Coumarin 343 as a standard λ_{ex} 400 nm. [b] Emission too weak to be measured.

cluded. The absorption spectra of the trinuclear complexes $PtPd_2$ (**5**) and Pt_3 (**6**) (Table 5) give two high-energy absorptions at 236 and 281 nm due to IL transitions and one shoulder that appears at 318 nm for complex **5** and which is slightly red-shifted for the triplatinum derivative **6** (332 nm) suggesting some degree of MLCT character.

The trinuclear complexes **5** and **6** do not show emissive properties. The remaining four complexes **1**–**4** exhibit luminescence to varying degrees. The mononuclear complex **1** exhibits a weak-structured emission only in CH_2Cl_2 glass at 77 K (427, 450, 465 nm) and in the solid state at 77 K (λ_{max} = 432 nm). The observed vibrational spacing ($\tilde{\nu}$ = 1190, 2052 cm^{-1}) can be attributed to a combination of vibrational modes of the C≡C and phenyl groups. The large Stokes shift of the emission from the corresponding singlet IL/MLCT transition and its lifetime (44 μs in the solid state, 77 K) is indicative of a triplet parentage, being attributed to a $^3\pi\pi^*$ excited state with a mixture of phenyl and acetylenic character, though a certain degree of metal perturbation can not be discarded.

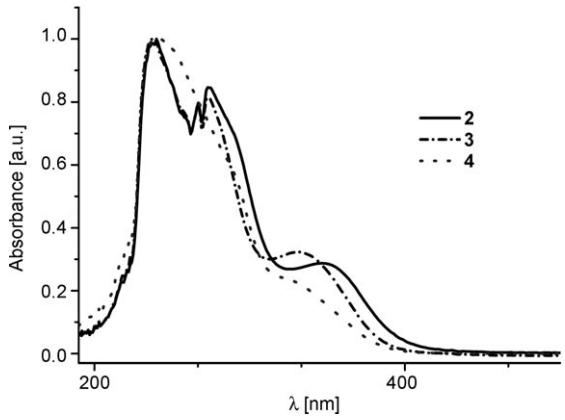

Figure 6. UV-visible spectra of the hexanuclear Pt_2M_4 complexes **2**–**4** in CH_2Cl_2 solution (5×10^{-5} M).

Excitation of solid hexanuclear complex [{PtCu$_2$(μ-C≡CPh)$_2$(μ-dmpz)$_2$}$_2$] (**2**) at 370 nm produces a bright yellowish-orange emission with λ_{max} at 570 nm both at 298 and 77 K. Upon excitation at lower energies (420 nm) at 298 K, the emission maximum is slightly red-shifted (580 nm) and a shoulder is detected at 565 nm. At 77 K, the profile of the emission is also more asymmetric if the excitation is performed at 400 nm (see Table 6). A similar behavior is observed in frozen CH_2Cl_2 glass (77 K) and, to illustrate this, the spectra obtained by increasing the excitation wavelength from 380 to 410 nm are shown in Figure 7. This behavior suggests the existence of ground-state heterogeneity[121] or, more likely, the presence of at least two closely lying emissive states. The emission lifetime data (see Table 6) indicate spin-forbidden processes showing lifetime values that increase upon cooling, consistent with a reduction in the nonradiative decay rates, as expected. By contrast, the emission

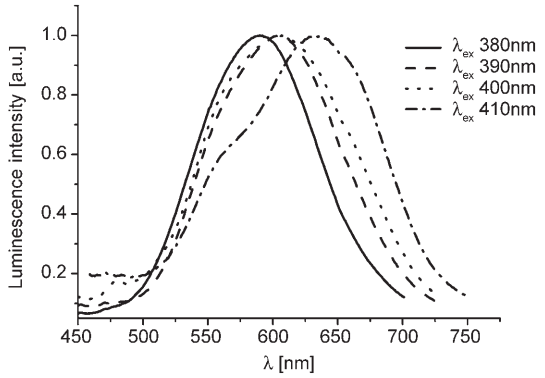

Figure 7. Normalized emission spectra of $[\{PtCu_2(\mu\text{-}C{\equiv}CPh)_2(\mu\text{-}dmpz)_2\}_2]$ **2** in CH_2Cl_2 solution (10^{-3} M) at 77 K with excitation wavelengths from 380 to 410 nm.

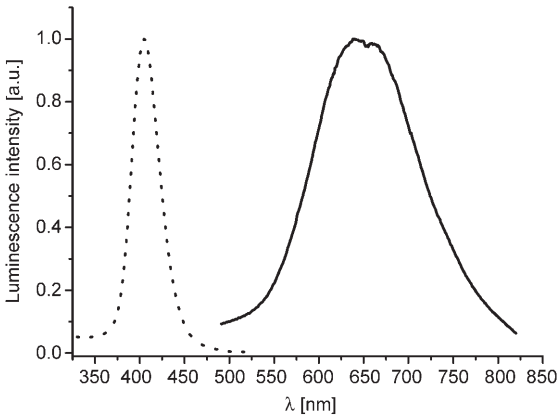

Figure 8. Normalized excitation (-----: $\lambda_{em}=640$ nm) and emission (——: $\lambda_{ex}=420$ nm) spectra of $[\{PtCu_2(\mu\text{-}C{\equiv}CPh)_2(\mu\text{-}dmpz)_2\}_2]$ **2** in CH_2Cl_2 solution (10^{-3} M) at 298 K.

profile in fluid solution (CH_2Cl_2) is not dependent on the wavelength.

Figure 8 shows both the emission ($\lambda_{max}=640$–660 nm) and excitation spectra ($\lambda_{max}=406$ nm) of complex **2** in ambient-temperature fluid solution. The excitation peak (406 nm) is red-shifted from the lowest spin-allowed absorption band (346 nm), in agreement with a predominantly triplet character. The remarkable red shift observed for the luminescence, going from a rigid medium (570 nm, solid; 590 nm, glass) to a solution (~650 nm) could be ascribed to the larger structural changes that may occur in solution than in the rigid lattice of the solid. This behaviour denoted as "rigidochromism" has been previously observed in several polynuclear copper,[137–139] gold,[140] and heteropolynuclear Pt–Cu[141] or Au–Cu[142] complexes. The assignment of the radiative excited state(s) is uncertain but the emission seems to be characteristic of the formation of the hexanuclear central core. With reference to previous work on heteropolynuclear Pt^{II}–copper(I) and -silver(I) alkynyl bridging complexes[5,25,94,120,133,135,136,141,143] the strong and enhanced phosphorescence relative to the precursor is associated to the η^2-platina alkyne [Pt-C≡CPh-Cu^I] entities. The emissive state is likely to derive from a ^{3}MLM′CT Pt(d)/π(C≡CPh)→Pt(p_z)/Cu(sp)/π*(C≡CPh) state modified by metal–metal interactions in view of the short Pt···Cu (3.016(9)–3.121(8) Å) contacts observed through the alkynyl bridging ligands.

The spectrum of the hexanuclear $[\{PtAg_2(\mu\text{-}C{\equiv}CPh)_2(\mu\text{-}dmpz)_2\}_2]$ (**3**) complex shows a strong structureless symmetrical band at 560 nm by excitation at 420 nm, and by excitation at higher energies (330–380 nm) luminesces to give a band at 550 nm with a shoulder at 480 nm. The excitation spectrum shows bands at 380 and 420 nm if the emission is monitored at the low-energy maximum (550 nm) and only the high-energy band (380 nm) if the emission is monitored at the high-energy shoulder (480 nm). Both bands are well-resolved upon cooling the solid at 77 K (see Table 6). Comparable behavior is observed when going from fluid CH_2Cl_2 solution (Figure 9) to glass (77 K) (Figure 10). As can be observed in Figure 10, in frozen CH_2Cl_2 glass (77 K), the emission is clearly resolved into two bands (470 and 580 nm) the

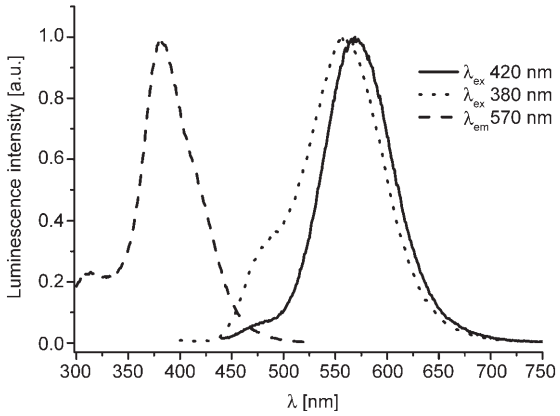

Figure 9. Normalized excitation and emission spectra of $[\{PtAg_2(\mu\text{-}C{\equiv}CPh)_2(\mu\text{-}dmpz)_2\}_2]$ **3** in CH_2Cl_2 solution (10^{-3} M) at 298 K.

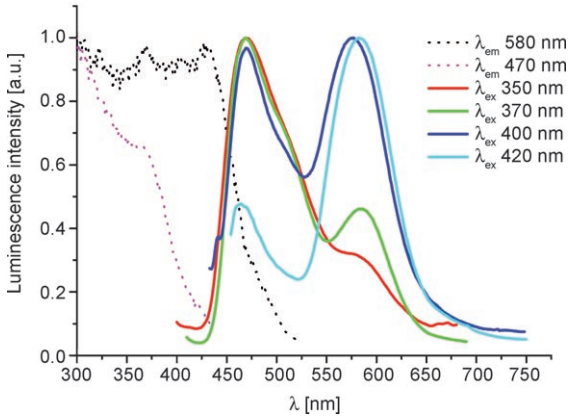

Figure 10. Normalized excitation (-----) and emission (——) spectra of $[\{PtAg_2(\mu\text{-}C{\equiv}CPh)_2(\mu\text{-}dmpz)_2\}_2]$ **3** in CH_2Cl_2 glass (10^{-3} M) at 77 K.

relative intensities of which depend on the excitation wavelength. The excitation profiles of both emissions are also different suggesting the existence of two low-lying emissive states. The lifetimes associated with both emissions are simi-

lar (17 μs, 480 nm; 16 μs, 570 nm, solid 77 K) and in the microsecond time scale are suggestive of a triplet-state origin. This behavior is not unexpected due to the presence of three different coordination environments for the silver centers ($Ag(\mu\text{-dmpz})_2$; $Ag(\mu\text{-dmpz})(\mu\text{-C}\equiv\text{CPh})$; $Ag(\mu\text{-C}\equiv\text{CPh})_2$) in the solid state (see Figure 3) and presumably in CH_2Cl_2 glass, which could lead to the existence of several emissive states. It is likely that the yellow, low-energy emission (560 nm, solid 298 K; 570 nm, solid 77 K) associated with the low-energy excitation (up to 460 nm) originates from emissive states derived from a ^{3}MLM′CT $Pt(d)/\pi(C\equiv CPh)\rightarrow Pt(p_z)/Ag(sp)/\pi^*(C\equiv CPh)$ state modified by Pt···Ag contacts (3.094(4) and 3.314(4) Å), as evidenced by the similarity of the emission with that of the hexanuclear cluster complex $[Pt_2Ag_4(C\equiv CPh)_8]$ ($\lambda_{em}=570$ nm, solid and CH_2Cl_2 solution at 298 K; 574 nm, solid 77 K, $\lambda_{ex}=445$ nm)[25,144] containing only alkynyl bridging ligands. The blue, high-energy emission at 470 nm, associated with the high-energy excitation (320–400 nm), is tentatively attributed to emissive states derived from pyrazolate-to-silver (or cluster) ^{3}LMCT transitions, probably mixed with metal d^{10} (d→s) character. By comparison, two blue emission bands (405 and 455 nm) and a green band (500 nm) have been recently reported for the dimer with pyrazolate bridging ligands [{3,5-$(CF_3)_2$Pz}Ag(2,4,6-collidine)].[63]

Unlike the hexanuclear complexes **2** and **3**, the related $[\{PtAu_2(\mu\text{-C}\equiv CPh)_2(\mu\text{-dmpz})_2\}_2]$ **4** that exhibits a similar structure to that of the platinum–silver congener **3**, is not emissive in the solid state at room temperature. The reason for the quenching of the luminescence is unclear at present. Upon cooling the solid (77 K), a weak, unstructured emission is detected at 590 nm upon excitation in the range 360–420 nm with a long-lived lifetime of 16 μs by using an excitation wavelength of 380 nm. Surprisingly, the intensity of the emission increases remarkably in fluid and frozen CH_2Cl_2 solutions. As was observed for the platinum–copper complex **2**, the emission is red-shifted in ambient-temperature fluid solution ($\lambda_{em}=622$ nm, CH_2Cl_2) by approximately 872 cm^{-1} from that observed in the solid state (77 K). As can be observed in Figure 11, a similar rigidochromism effect is seen upon freezing the CH_2Cl_2 solution at cryogenic temperatures (77 K). However in rigid glass, in addition to a broad low-energy emission at 575 nm, comparable to that observed in the solid state (590 nm, 77 K), a distinctive high-energy vibronic band emerges (λ = 446 (max), 475 nm (sh)). The vibrational spacing of 1370 cm^{-1} of this latter band corresponds to the C=N and/or N=N vibrations of the pyrazolate-based ligand and is tentatively ascribed mainly to LMCT $\pi(dmpz)\rightarrow Au^I$ transitions. Similar structured emissions have been reported for other terminal or bridging pyrazolate gold complexes.[58,59,64,111] As in complexes **2** and **3**, the low-energy emission is associated with the η^2-coordination of the platina alkyne $Pt(C\equiv CPh)\rightarrow Au^I$ entities and assigned to a similar MLM′CT transition. As a comparison, the emission and excitation spectra of the three complexes **2**–**4** in fluid CH_2Cl_2 (298 K) are shown in Figure 12. Curiously, the emission maxima follow the decreasing energy order Ag > Au > Cu, while the excitation maxima follow the order Au ≈ Ag > Cu, similar to that observed in the absorption spectra. Finally, we note that the radiative quantum yield measured at room temperature in CH_2Cl_2 solution is comparable in the platinum–copper **2** and platinum–gold **4** complexes and increases notably in the platinum–silver one **3**.

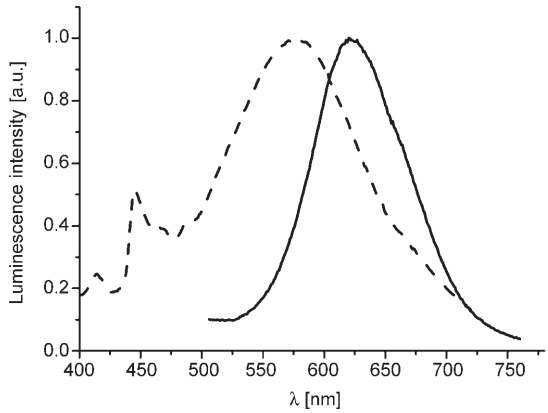

Figure 11. Normalized emission spectra of $[\{PtAu_2(\mu\text{-C}\equiv CPh)_2(\mu\text{-dmpz})_2\}_2]$ **4** in CH_2Cl_2 solution (10^{-3} M) (——: 298 K, $\lambda_{ex}=390$ nm; -----: 77 K, $\lambda_{ex}=370$ nm).

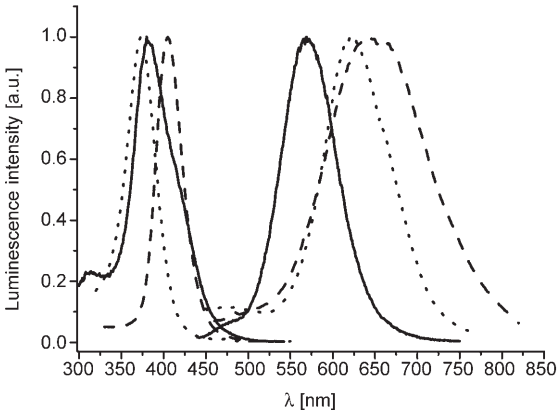

Figure 12. Normalized emission (right) and excitation (left) spectra of complexes **2**–**4** in fluid CH_2Cl_2 solution (10^{-3} M) at 298 K: **2** (-----: $\lambda_{ex}=420$ nm, $\lambda_{em}=640$ nm); **3** (——: $\lambda_{ex}=420$ nm, $\lambda_{em}=560$ nm); **4** (•••••: $\lambda_{ex}=370$ nm, $\lambda_{em}=620$ nm).

Conclusion

This work describes the synthesis of *cis*-$[Pt(C\equiv CPh)_2(Hdmpz)_2]$ (**1**) and its use as a precursor for the preparation of homo- and heteropolynuclear complexes. Double deprotonation of complex **1** with readily available M^I (M = Cu, Ag, Au) species affords the corresponding neutral fragments $PtM_2(\mu\text{-C}\equiv CPh)_2(\mu\text{-dmpz})_2$ in excellent (complexes **2**, **3**) or moderate (complex **4**) yields, and their structures as determined by X-ray diffraction reveal that they dimerize forming discrete clusters $[\{PtM_2(\mu\text{-C}\equiv CPh)_2(\mu\text{-dmpz})_2\}_2]$ **2**–**4**. X-

ray data show that in the three complexes the two Pt(C≡CPh)$_2$(dmpz)$_2$ fragments are connected by four d^{10} metal centers that are stabilized by alkynyl and dimethylpyrazolyl bridging ligands. However, while in the platinum–copper derivative [{PtCu$_2$(μ-C≡CPh)$_2$(μ-dmpz)$_2$}$_2$] **2**, all copper centers exhibit similar local geometry, being linearly coordinated to a nitrogen atom and η^2 to one alkynyl fragment, in the related platinum–silver (**3**) and platinum–gold (**4**) derivatives the silver and gold atoms present three different coordination environments. Two of the atoms show similar local coordination to the copper centers in derivative **2** while the other two are stabilized by two nitrogen atoms (from two bridging dmpz ligands) and two η^2-alkynyl fragments, respectively. The study of their photophysical properties produces interesting results. The hexanuclear complexes exhibit bright luminescence with moderate quantum yields in fluid solution. Dual long-lived emission is observed in all complexes, being clearly resolved in low-temperature rigid media (solid state and CH_2Cl_2 glass). The low-energy emission is associated with the η^2-platina alkyne (Pt-C≡CPh-d^{10}) entities and is ascribed to the MLM′CT Pt(d)/π(C≡CPh)→Pt(p_z)/M′(sp)/π*-(C≡CPh) transition modified by metal–metal interactions in view of the relatively short Pt···M′ (d^{10}) contacts. The high energy emission that appears at 470 nm (glass) in [{PtAg$_2$(μ-C≡CPh)$_2$(μ-dmpz)$_2$}$_2$] **3** and is clearly structured in the platinum–gold derivative [{PtAu$_2$(μ-C≡CPh)$_2$(μ-dmpz)$_2$}$_2$] **4**, with a vibronic progression related to the C=N and/or N=N vibrations, is attributed to emissive states derived from dimethylpyrazolate-to-metal′ (d^{10}) LM′CT transitions π(dmpz)→M′(d^{10}). In fluid solution, the emission band related to the MLM′CT transition follows the energy order Ag > Au > Cu. Trinuclear $PtPd_2$ and Pt_3 complexes stabilized by heterobridged-dmpz/C≡CPh are also easily generated but they do not show luminescent properties. An extension of this chemistry to different alkynyl and pyrazolate ligands is in progress.

Experimental Section

General procedures and materials: Elemental analyses were carried out in a Perkin–Elmer 240-B microanalyser. IR spectra were recorded on a Perkin–Elmer 599 spectrophotometer (Nujol mulls between polyethylene plates in the range 350–4000 cm^{-1}). NMR spectra were recorded on a Varian Unity-300 spectrometer by using the standard references. Mass spectral analyses were performed with a VG Autospec instrument. UV-visible spectra were obtained on a Hewlett–Packard 8453 spectrometer. Emission and excitation spectra were obtained on a Perkin–Elmer luminescence spectrometer LS 50B and on a Jobin–Yvon Horiba Fluorolog 3–11 Tau-3 spectrofluorimeter, in which the lifetime measurements were performed operating in the phosphorimeter mode. The solution emission quantum yields were measured by the Demas and Crosby method[145] by using Coumarin 343 in degassed ethanol as a standard. 3,5-Dimethylpyrazole (Hdmpz) was purchased from Aldrich and phenylacetylene was purchased from Merck. [Cu(MeCN)$_4$]PF$_6$,[146] PPN[Au(acac)$_2$],[147] $AgClO_4$, [M(C^P)(O$_2$CCH$_3$)]$_2$ (M = Pd,[148] Pt[78]) were prepared by literature methods.

***cis*-[PtCl$_2$(Hdmpz)$_2$] (A)**: A suspension of $PtCl_2$ (0.397 g, 1.49 mmol) and Hdmpz (0.287 g, 2.99 mmol) was heated under reflux for 90 min. The mixture was then filtered and the solution evaporated to dryness. Et_2O (10 mL) was added to the residue to give compound **A** (0.563 g, 82%). ^{1}H NMR (300 MHz, CD_2Cl_2, 20 °C, TMS): δ = 2.17 (s, 6H; Me), 2.38 (s, 6H; Me), 5.76 (s, 2H; H^4), 12.11 ppm (s, 2H; NH); elemental analysis calcd (%) for $C_{10}Cl_2H_{16}N_4Pt$: C 26.10; H 3.49; N 12.22; found: C 26.14; H 3.16; N 11.96.

***cis*-[Pt(C≡CPh)$_2$(Hdmpz)$_2$] (1)**: A solution of LiC≡CPh (5 mmol), prepared by treating HC≡CPh (0.57 mL, d = 0.93 g mL^{-1}, 97%, 5 mmol) in Et_2O (10 mL) with Li*n*Bu (2 mL, 2.5 M, 5 mmol) in Et_2O (5 mL) at −10 °C under an argon atmosphere, was stirred for 15 min and then *cis*-[PtCl$_2$(Hdmpz)$_2$] (**A**) (0.573 g, 1.25 mmol) and Et_2O (10 mL) were added. The mixture was allowed to reach RT and was stirred for 14 h. The resulting mixture was evaporated to dryness. $CHCl_3$ (50 mL) was added to the residue, the mixture was filtered through Celite, and the solution was evaporated to dryness. Addition of Et_2O (10 mL) afforded a solid that was filtered, washed with acetone (2 × 10 mL), and dried. Compound **1** was obtained as an air-stable, beige solid (0.383 g, 52%). ^{1}H NMR (300 MHz, CD_2Cl_2, 20 °C, TMS): δ = 1.41 (s, 3H; Me), 1.87 (s, 3H; Me), 2.05 (s, 3H; Me), 2.70 (s, 3H; Me), 5.65 (s, 1H; H^4), 5.86 (s, 1H; H^4), 7.40–6.90 (m, 10H; Ph), 11.71 (s, 1H; NH), 12.99 ppm (s, 1H; NH); IR (Nujol): $\tilde{\nu}$ = 3216 (N–H), 2127, 2115 cm^{-1} (C≡C); MS (FAB$^+$): *m*/*z* (%): 584 (85) [M^+], 483 (45) [M^+−C_2Ph], 386 (100) [Pt(dmpz)$_2$H$^+$]; elemental analysis calcd (%) for $C_{26}H_{26}N_4Pt$: C 52.98; H 4.41; N 9.50; found: C 52.72; H 4.43; N 9.88.

[{PtCu$_2$(μ-C≡CPh)$_2$(μ-dmpz)$_2$}$_2$] (2): Compound **1** (0.208 g, 0.35 mmol) and NEt_3 (1.5 mL) were added to a colorless solution of [Cu(CH$_3$CN)$_4$]PF$_6$ (0.262 g, 0.70 mmol) in CH_2Cl_2 (20 mL) under an argon atmosphere. The mixture was stirred at RT for 2 h and the resulting orange solution was evaporated to dryness. Addition of dry Et_2O (80 mL) to the residue gave a yellow solution that was filtered through Celite under argon. The solution was evaporated to dryness and the addition of cold methanol (10 mL) afforded a yellow solid that was filtered off and vacuum dried (0.227 g, 90%). ^{1}H NMR (300 MHz, $CDCl_3$, 20 °C, TMS): δ = 1.74 (s, 6H; Me), 1.80 (s, 6H; Me), 2.01 (s, 6H; Me), 2.48 (s, 6H; Me), 5.71 (s, 2H; H^4), 5.78 (s, 2H; H^4), 6.80–7.50 ppm (m, 20H; Ph); IR (Nujol): $\tilde{\nu}$ = 2023, 1984 cm^{-1} (C≡C); (CH_2Cl_2, 296 K): $\tilde{\nu}$ = 2026, 1989 cm^{-1} (C≡C); MS (FAB$^+$): *m*/*z* (%): 1428 (100) [M^+], 1334 (75) [M^+−dmpz]; elemental analysis calcd (%) for $Pt_2Cu_4C_{52}H_{48}N_8$: C 43.70, H 3.39, N 7.84; found: C 43.68, H 3.20, N 7.65.

[{PtAg$_2$(μ-C≡CPh)$_2$(μ-dmpz)$_2$}$_2$] (3): $AgClO_4$ (0.090 g, 0.44 mmol) and NEt_3 (1.5 mL) were added to a solution of compound **1** (0.127 g, 0.215 mmol) in CH_2Cl_2/Et_2O (30:10 mL). The mixture was stirred at RT for 4 h in the dark. The yellow solution, filtered through paper, was evaporated to dryness. Addition of Et_2O (40 mL) to the residue gave a yellow solution that was filtered through Celite. The solvent was removed and the addition of cold methanol (10 mL) afforded a yellow solid that was filtered off and vacuum dried (0.138 g, 80%). ^{1}H NMR (300 MHz, $CDCl_3$, 20 °C, TMS): δ = 1.90 (s, 12H; Me), 2.29 (s, 12H; Me), 5.85 (s, 4H; H^4), 7.00–7.50 ppm (m, 20H; Ph); IR (Nujol): $\tilde{\nu}$ = 2039 cm^{-1} (C≡C); (CH_2Cl_2, 296 K): $\tilde{\nu}$ = 2043 cm^{-1} (C≡C); MS (FAB$^+$): *m*/*z* (%): 1607 (75) [M^+], 1512 (80) [M^+−dmpz]; elemental analysis calcd (%) for $Pt_2Ag_4C_{52}H_{48}N_8$: C 38.88, H 2.98, N 6.97; found: C 38.70, H 2.87, N 6.78.

[{PtAu$_2$(μ-C≡CPh)$_2$(μ-dmpz)$_2$}$_2$] (4): Compound **1** (0.105 g, 0.18 mmol) and NEt_3 (1.5 mL) were added to a colorless solution of PPN[Au(acac)$_2$] (PPN: $Ph_2P{=}N^+{=}PPh_3$) (0.331 g, 0.36 mmol) in CH_2Cl_2 (20 mL) under an argon atmosphere. The mixture was stirred at 0 °C for 2 h and the resulting solution was evaporated to dryness. Addition of cold methanol (20 mL, 0 °C) afforded a beige solid that was filtered off, was recrystallized by Et_2O/MeOH (60:10 mL), and was vacuum dried to give compound **4** (0.081 g, 46%). ^{1}H NMR (300 MHz, CD_2Cl_2, 293 K): δ = 2.02 (s, 6H; Me), 2.06 (s, 6H; Me), 2.21 (s, 6H; Me), 2.54 (s, 6H; Me), 5.9 (s, 2H; H^4), 6.03 (s, 2H; H^4), 7.6–7.1 ppm (m, 20H; Ph); IR (Nujol): $\tilde{\nu}$ = 1948 cm^{-1} (C≡C); (CH_2Cl_2, 296 K): $\tilde{\nu}$ = 1959 cm^{-1} (C≡C); MS (FAB$^+$): *m*/*z* (%): 1963 (15) [M^+]; elemental analysis calcd (%) for $Pt_2Au_4C_{52}H_{48}N_8$: C 31.82, H 2.44, N 5.70; found: C 31.78, H 2.40, N 5.89.

[Pt(μ-C≡CPh)$_2$(μ-dmpz)$_2$Pd$_2$(C^P)$_2$] (5): [{Pd(C^P)(μ-O$_2$CCH$_3$)}$_2$] (0.151 g, 0.16 mmol) and NEt_3 (1.5 mL) were added to a solution of compound **1** (0.100 g, 0.16 mmol) in CH_2Cl_2 (20 mL). The mixture was stirred at RT for 5 h and the resulting solution was evaporated to dryness. Addi-

tion of cold methanol (30 mL, 0 °C) to the residue rendered a yellow solid that was filtered off and vacuum dried (0.168 g, 75 %). ^{1}H NMR (300 MHz, CD_2Cl_2, 293 K): $\delta = 1.79$ (s, 6H; Me, dmpz), 2.22 (s, 6H; Me, C^P), 2.43 (s, 6H; Me, dmpz), 2.81 (s, 6H; Me, C^P), 3.79 (ν_A), 3.87 (ν_B) ($J_{A,B} =$ 12.9 Hz, 4H; CH_2, C^P), 5.84 (s, 2H; H^4, dmpz), 6.70–7.70 ppm (m, 34H; C_2Ph, C^P); ^{31}P NMR (300 MHz, CD_2Cl_2, 293 K): $\delta = 43.73$ ppm; IR (Nujol): $\tilde{\nu} = 2055$ cm^{-1}(C≡C); MS (FAB$^+$): *m*/*z* (%): 1407 (25) [*M*$^+$]; elemental analysis calcd (%) for $Pt_1Pd_2P_2C_{68}H_{64}N_4$: C 58.06, H 4.55, N 3.98; found: C 58.00 H 4.30, N 3.91.

[Pt(μ-C≡CPh)$_2$(μ-dmpz)$_2$Pt$_2$(C^P)$_2$] (6): A pale yellow solution of compound **1** (0.153 g, 0.26 mmol) in CH_2Cl_2 (20 mL) was treated with [{Pt(C^P)(μ-O_2CCH_3)}$_2$] (0.290 g, 0.26 mmol) and NEt_3 (1.5 mL) and was stirred for 17 h at RT. The solvent was then removed and cold methanol (30 mL, 0 °C) was added to afford a beige solid that was filtered off and vacuum dried (0.350 g, 85 %). ^{1}H NMR (300 MHz, CD_2Cl_2, 293 K): $\delta = 1.88$ (s, 6H; Me, dmpz), 2.15 (s, 6H; Me, C^P), 2.46 (s, 6H; Me, dmpz), 2.81 (s, 6H; Me, C^P), 3.69 (ν_A), 3.94 (ν_B) ($J_{A,B} = 16$ Hz, 4H; CH_2, C^P), 5.89 (s, 2H; H^4, dmpz), 6.60–8.00 ppm (m, 34H; C_2Ph, C^P); IR (Nujol): $\tilde{\nu} = 2029$, 1989 cm^{-1}(C≡C); ^{31}P NMR (300 MHz, CD_2Cl_2, 293 K): $\delta = 25.45$ (s, $J_{Pt,P} = 4069$ Hz); MS (FAB$^+$): *m*/*z* (%): 1584 (65) [*M*$^+$]; elemental analysis calcd (%) for $Pt_3P_2C_{68}H_{64}N_4$: C 51.56, H 4.04, N 3.53; found: C 51.32, H 4.06, N 3.65.

X-ray structure determinations: Crystal data and other details of the structure analyses are presented in Table 7. Crystals suitable for X-ray diffraction studies were obtained as indicated in each synthesis procedure. Crystals were mounted on the end of a quartz fiber. The radiation used in all cases was graphite monochromated $Mo_{K\alpha}$ ($\lambda = 0.71073$ Å). For **1**, **2**, and **6**·CH_2Cl_2 X-ray intensity data were collected on a Bruker Smart Apex diffractometer. The diffraction frames were integrated by using the SAINT program.[149] For **3**·2 Me_2CO and **4**·2 Me_2CO X-ray intensity data were collected on an Oxford Diffraction Xcalibur diffractometer. The diffraction frames were integrated by using the CrysAlis RED program.[150] In all cases, the sets of data were corrected for absorption with SADABS.[151] The structures were solved by Patterson and Fourier methods, and were refined by full-matrix least-squares on F^2 with SHELXL-97.[152] All non-hydrogen atoms were assigned anisotropic displacement parameters and were refined without positional constraints except as noted below. All hydrogen atoms were constrained to idealized geometries and assigned isotropic displacement parameters equal to 1.2 times the U_{iso} values of their attached parent atoms (1.5 times for the methyl hydrogen atoms). In the structure of **4**·2 Me_2CO, the carbon atoms of the phenyl group of one of the phenylacetylide ligands were disordered over two sets of positions that were refined with partial occupancy 0.55/0.45. These rings were refined as rigid groups, with analogous atoms sharing common isotropic thermal parameters. Full-matrix least-squares refinement of these models against F^2 converged to the final residual indices given in Table 7.

CCDC 296469–296473 contain the supplementary crystallographic data for this paper. These data can be obtained free of charge from The Cambridge Crystallographic Data Centre via www.ccdc.cam.ac.uk/data_request/cif.

Table 7. Crystal data and structure refinement for complexes **1**, **2**, **3**·2 Me_2CO, **4**·2 Me_2CO, and **6**·CH_2Cl_2.

	1	**2**	**3**·2 Me_2CO	**4**·2 Me_2CO	**6**·CH_2Cl_2
formula	$C_{26}H_{26}N_4Pt$	$C_{52}H_{48}N_8Cu_4Pt_2$	$C_{52}H_{48}N_8Ag_4Pt_2$ ·2 Me_2CO	$C_{52}H_{48}N_8Au_4Pt_2$ ·2 Me_2CO	$C_{68}H_{64}N_4P_2Pt_3$ ·CH_2Cl_2
M_w [g mol^{-1}]	589.60	1429.32	1722.80	2079.19	1669.37
T [K]	100(1)	100(1)	100(1)	100(1)	100(1)
λ [Å]	0.71073	0.71073	0.71073	0.71073	0.71073
crystal system	orthorhombic	monoclinic	monoclinic	monoclinic	triclinic
space group	*Pbcn*	$P2_1/c$	*C*2/*c*	*C*2/*c*	$P\bar{1}$
a [Å]	13.1703(8)	12.5559(7)	26.0674(6)	25.9885(5)	15.589(3)
b [Å]	17.9500(10)	15.7183(8)	22.4954(6)	22.6811(3)	19.796(4)
c [Å]	19.6663(11)	25.1124(14)	10.6955(2)	10.5855(2)	20.948(4)
α [°]	90	90	90	90	82.306(3)
β [°]	90	90.134(1)	114.118(2)	113.741(2)	79.919(3)
γ [°]	90	90	90	90	75.337(3)
V [Å^3]	4649.2(5)	4956.1(5)	5724.3(2)	5711.6(2)	6130.1(19)
Z	4	4	4	4	2
ρ [g cm^{-3}]	1.685	1.916	1.999	2.418	1.809
μ [mm^{-1}]	6.056	7.353	6.259	15.164	7.014
F(000)	2304	2752	3296	3808	3224
2θ range [°] ($\pm h$,$\pm k$,$\pm l$)	3.8–50.0	3.1–50.1	5.2–50.1	4.0–50.1	3.3–50.0
final R indices [$I > 2\sigma(I)$][a]					
R_1	0.0186	0.0327	0.0250	0.0274	0.0328
wR_2	0.0478	0.0531	0.0603	0.0644	0.0782
R indices (all data)					
R_1	0.0230	0.0528	0.0280	0.0313	0.0411
wR_2	0.0488	0.0554	0.0618	0.0662	0.0824
goodness-of-fit on F^2[b]	1.018	1.011	1.063	1.057	1.015

[a] $R_1 = \Sigma(|F_o| - |F_c|)/\Sigma|F_o|$. $wR_2 = [\Sigma w(F_o^2 - F_c^2)^2/\Sigma w(F_o^2)^2]^{1/2}$. [b] Goodness-of-fit $= [\Sigma w(F_o^2 - F_c^2)^2/(n_{obs} - n_{param})]^{1/2}$.

Acknowledgements

This work was supported by the Spanish MCYT (DGI)/FEDER (Project CTQ2005-08606-C02-01, 02) and the Gobierno de Aragón (Grupo de Excelencia: Química Inorgánica y de los Compuestos Organometálicos).

[1] M. I. Bruce, *Chem. Rev.* **1998**, *98*, 2797.
[2] H. Lang, D. S. A. George, G. Rheinwald, *Coord. Chem. Rev.* **2000**, *206–207*, 101.
[3] U. Rosenthal, P. M. Pellny, F. G. Kirchbauer, V. V. Burlakov, *Acc. Chem. Res.* **2000**, *33*, 119.
[4] U. M. Miskoski, Y. Li, K.-K. Cheung, *J. Am. Chem. Soc.* **2001**, *123*, 4985.
[5] V. W. W. Yam, *Acc. Chem. Res.* **2002**, *35*, 555, and references therein.
[6] M. Hissler, J. E. McGarrah, W. B. Connick, D. K. Geiger, S. D. Cummings, R. Eisenberg, *Coord. Chem. Rev.* **2000**, *208*, 115.
[7] U. Rosenthal, *Angew. Chem.* **2003**, *115*, 1838; *Angew. Chem. Int. Ed.* **2003**, *42*, 1794.
[8] N. J. Long, C. K. Williams, *Angew. Chem.* **2003**, *115*, 2690; *Angew. Chem. Int. Ed.* **2003**, *42*, 2586.
[9] J. E. McGarrah, R. Eisenberg, *Inorg. Chem.* **2003**, *42*, 4355.
[10] M. I. Bruce, K. Costuas, J. F. Halet, B. C. Hall, P. J. Low, B. K. Nicholson, B. W. Skelton, A. J. White, *J. Chem. Soc. Dalton Trans.* **2002**, 383.
[11] E. Bosch, C. L. Barnes, *Organometallics* **2000**, *19*, 5522.
[12] K. Onitsuka, A. Luchi, M. Fujimoto, S. Takahashi, *Chem. Commun.* **2001**, 741.
[13] R. Ziessel, M. Hissler, A. El-ghayoury, A. Harriman, *Coord. Chem. Rev.* **1998**, *178–180*, 1251.
[14] D. K. C. Tears, D. R. McMillin, *Coord. Chem. Rev.* **2001**, *211*, 195.

[15] S. Back, M. Albrecht, A. L. Speck, G. Rheinwald, H. Lang, G. van Koten, *Organometallics* **2001**, *20*, 1024.
[16] I. R. Whittall, A. M. McDonagh, M. G. Humphrey, M. Samok, *Adv. Organomet. Chem.* **1998**, *42*, 291.
[17] Y. Liu, S. Jiang, K. Glusac, D. H. Powell, D. F. Anderson, K. S. Schanze, *J. Am. Chem. Soc.* **2002**, *124*, 12412.
[18] N. J. Long, A. J. P. White, D. J. Williams, M. Younus, *J. Organomet. Chem.* **2002**, *649*, 94.
[19] H. Hayashi, K. Onitsuka, N. Kobayashi, S. Takahashi, *Angew. Chem.* **2001**, *113*, 4216; *Angew. Chem. Int. Ed.* **2001**, *40*, 4092.
[20] P. Siemsen, U. Gubler, C. Bosshard, P. Günter, F. Diederich, *Chem. Eur. J.* **2001**, *7*, 1333.
[21] M. S. Khan, M. R. A. Al-Mandhary, M. K. Al-Suti, A. K. Hisahm, P. R. Raithby, B. Ahrens, M. F. Mahon, L. Male, E. A. Marseglia, E. Tedesco, R. H. Friend, A. Köhler, N. Feeder, S. J. Teat, *J. Chem. Soc. Dalton Trans.* **2002**, 1358, and references therein.
[22] K. M. C. Wong, C. K. Hui, K.-L. Yu, V. W. W. Yam, *Coord. Chem. Rev.* **2002**, *229*, 123.
[23] V. W. W. Yam, K. K. W. Lo, K. M. C. Wong, *J. Organomet. Chem.* **1999**, *578*, 3.
[24] V. W. W. Yam, C. K. Hui, K. M. C. Wong, N. Zhu, K. K. Cheung, *Organometallics* **2002**, *21*, 4326.
[25] J. P. H. Chartman, J. Forniés, J. Gómez, E. Lalinde, R. I. Merino, M. T. Moreno, A. G. Orpen, *Organometallics* **1999**, *18*, 3353.
[26] I. Ara, J. Forniés, J. Gómez, E. Lalinde, M. T. Moreno, *Organometallics* **2000**, *19*, 3137.
[27] I. Ara, J. R. Berenguer, J. Forniés, J. Gómez, E. Lalinde, A. Martín, R. I. Merino, *Inorg. Chem.* **1997**, *36*, 6461.
[28] J. R. Berenguer, J. Forniés, J. Gómez, E. Lalinde, M. T. Moreno, *Organometallics* **2001**, *20*, 4847, and references therein.
[29] J. P. H. Charmant, J. Forniés, J. Gómez, E. Lalinde, R. I. Merino, M. T. Moreno, A. G. Orpen, *Organometallics* **2003**, *22*, 652.
[30] J. Forniés, J. Gómez, E. Lalinde, M. T. Moreno, *Inorg. Chem.* **2001**, *40*, 5415.
[31] J. R. Berenguer, J. Forniés, B. Gil, E. Lalinde, *Chem. Eur. J.* **2005**, *11*, 1.
[32] S. Trofimenko, *Prog. Inorg. Chem.* **1986**, *34*, 115.
[33] A. P. Sadimenko, S. S. Basson, *Coord. Chem. Rev.* **1996**, *147*, 247.
[34] G. La Monica, G. A. Ardizzoia, *Prog. Inorg. Chem.* **1997**, *46*, 151.
[35] A. P. Sadimenko, *Adv. Heterocycl. Chem.* **2001**, *80*, 157.
[36] G. A. Ardizzoia, S. Cenini, G. La Monica, N. Masciocchi, A. Maspero, M. Moret, *Inorg. Chem.* **1998**, *37*, 4284.
[37] N. Masciocchi, M. Moret, P. Cairati, A. Sironi, G. A. Ardizzoia, G. La Monica, *J. Am. Chem. Soc.* **1994**, *116*, 7668.
[38] H. V. R. Dias, S. A. Polach, Z. Wang, *J. Fluorine Chem.* **2000**, *103*, 163.
[39] R. G. Raptis, J. P. Fackler Jr., *Inorg. Chem.* **1988**, *27*, 4179.
[40] M. K. Ehlert, S. J. Rettig, A. Storr, R. C. Thompson, J. Trotter, *Can. J. Chem.* **1990**, *68*, 1444.
[41] M. K. Ehlert, S. J. Rettig, A. Storr, R. C. Thompson, J. Trotter, *Can. J. Chem.* **1992**, *70*, 2161.
[42] M. K. Ehlert, A. Storr, D. A. Summers, R. C. Thompson, *Can. J. Chem.* **1997**, *75*, 491.
[43] H. H. Murray, R. G. Raptis, J. P. Fackler Jr., *Inorg. Chem.* **1988**, *27*, 26.
[44] F. Meyer, A. Jacobi, L. Zsolnai, *Chem. Ber.* **1997**, *130*, 1441.
[45] B. Bovio, F. Bonati, G. Banditelli, *Inorg. Chim. Acta* **1984**, *87*, 25.
[46] R. G. Raptis, H. H. Murray, J. P. Fackler Jr., *Acta Crystallogr. Sect. C.* **1988**, *44*, 970.
[47] R. G. Raptis, J. P. Fackler Jr., *Inorg. Chem.* **1990**, *29*, 5003.
[48] J. Barberá, A. Elduque, R. Giménez, F. J. Lahoz, J. A. López, L. A. Oro, J. L. Serrano, *Inorg. Chem.* **1998**, *37*, 2960.
[49] G. Yang, R. G. Raptis, *Inorg. Chem.* **2003**, *42*, 261.
[50] M. C. Torralba, P. Ovejero, M. J. Mayoral, M. Cano, J. A. Campo, J. V. Heras, E. Pinilla, M. R. Torres, *Helv. Chim. Acta* **2004**, *87*, 250.
[51] P. Baran, C. M. Marrero, S. Pérez, R. G. Raptis, *Chem. Commun.* **2002**, 1012.
[52] K. Umakoshi, Y. Yamauchi, K. Nakamiya, T. Kojima, M. Yamasaki, H. Kawano, M. Onishi, *Inorg. Chem.* **2003**, *42*, 3907.
[53] W. Burger, J. Strähle, *Z. Anorg. Allg. Chem.* **1985**, *529*, 111.
[54] J. Forniés, A. Martín, V. Sicilia, L. F. Martín, *Chem. Eur. J.* **2003**, *9*, 3427.
[55] G. A. Ardizzoia, G. La Monica, S. Cenini, M. Moret, N. Masciocchi, *J. Chem. Soc. Dalton Trans.* **1996**, 1351.
[56] H. V. R. Dias, H. V. K. Diyabalanage, M. G. Eldabaja, O. Elbejeirami, M. A. Rawashdeh-Omary, M. A. Omary, *J. Am. Chem. Soc.* **2005**, *127*, 7489.
[57] M. A. Omary, M. A. Rawashdeh-Omary, M. W. A. Gonser, O. Elbjeirami, T. Grimes, T. R. Cundari, H. V. K. Diyabalanage, C. S. P. Gamage, H. V. R. Dias, *Inorg. Chem.* **2005**, *44*, 8200.
[58] A. A. Mohamed, T. Grant, R. J. Staples, J. P. Fackler Jr., *Inorg. Chim. Acta* **2004**, *357*, 1761.
[59] P. Ovejero, M. Cano, J. A. Campo, J. V. Heras, A. Laguna, O. Crespo, E. Pinilla, M. R. Torres, *Helv. Chim. Acta* **2004**, *87*, 2057.
[60] K. Singh, J. R. Long, P. Stavropoulos, *J. Am. Chem. Soc.* **1997**, *119*, 2942.
[61] A. Kishimura, T. Yamashita, T. Aida, *J. Am. Chem. Soc.* **2005**, *127*, 179.
[62] B. Ma, J. Li, P. I. Djurovich, M. Yousufuddin, R. Bau, M. E. Thompson, *J. Am. Chem. Soc.* **2005**, *127*, 28.
[63] M. A. Omary, M. A. Rawashdeh-Omary, H. V. K. Diyabalanage, H. V. R. Dias, *Inorg. Chem.* **2003**, *42*, 8612.
[64] A. A. Mohamed, J. M. López de Luzuriaga, J. P. Fackler Jr., *J. Clust. Sci.* **2003**, *14*, 61.
[65] M. Enomoto, A. Kishimura, T. Aida, *J. Am. Chem. Soc.* **2001**, *123*, 5608.
[66] S. W. Lai, M. C. W. Chan, K. K. Cheung, S. M. Peng, C. M. Che, *Organometallics* **1999**, *18*, 3991.
[67] S. Fernández, J. Forniés, B. Gil, J. Gómez, E. Lalinde, *Dalton Trans.* **2003**, 822.
[68] S. C. Chan, M. C. W. Chan, Y. Wang, C. M. Che, K. K. Cheung, N. Zhu, *Chem. Eur. J.* **2001**, *7*, 4180.
[69] J. E. McGarrah, Y.-J. Kim, M. Hissler, R. Eisenberg, *Inorg. Chem.* **2001**, *40*, 4510.
[70] C. E. Whittle, J. A. Weinstein, M. W. George, K. S. Schanze, *Inorg. Chem.* **2001**, *40*, 4053.
[71] K. M. C. Wong, W. S. Tang, B. W. K. Chu, N. Zhu, V. W. W. Yam, *Organometallics* **2004**, *23*, 3459.
[72] C. J. McAdam, E. J. Blackie, J. L. Morgan, S. A. Mole, B. H. Robinson, J. Simpson, *J. Chem. Soc. Dalton Trans.* **2001**, 2362.
[73] M. A. Cinellu, S. Stoccoro, G. Minghetti, A. L. Bandini, G. Banditelli, B. Bovio, *J. Organomet. Chem.* **1989**, *372*, 311.
[74] W. Burger, J. Strähle, *Z. Anorg. Allg. Chem.* **1986**, *539*, 27.
[75] A. B. Goel, S. Goel, D. Vanderveer, *Inorg. Chim. Acta* **1984**, *82*, L9.
[76] V. K. Jain, S. Kannan, E. R. T. Tiekink, *J. Chem. Soc. Dalton Trans.* **1993**, 3625.
[77] A. Singhal, V. K. Jain, R. P. Patel, A. Vyas, R. Bohra, *J. Organomet. Chem.* **1994**, *479*, 87.
[78] L. R. Falvello, J. Forniés, A. Martín, V. Sicilia, P. Villarroya, *Organometallics* **2002**, *21*, 4604.
[79] P. Espinet, J. Forniés, E. Lalinde, F. Martínez, M. T. Moreno, A. Ruiz, M. Tomás, A. J. Welch, *J. Chem. Soc. Dalton Trans.* **1990**, 791.
[80] H. Lang, A. del Villar, B. Walfort, *Inorg. Chem. Commun.* **2004**, *7*, 694.
[81] J. Forniés, M. A. Gómez-Saso, E. Lalinde, F. Martínez, M. T. Moreno, *Organometallics* **1992**, *11*, 2873.
[82] M. Nardelli, *Comput. Chem.* **1983**, *7*, 95.
[83] X. Solans, J. Solans, C. Miravitlles, D. Miguel, V. Riera, J. M. Rubio-González, *Acta Crystallogr. Sect. C* **1986**, *42*, 975.
[84] F. Olbrich, G. Schmidt, E. Weiss, U. Behrens, *J. Organomet. Chem.* **1993**, *456*, 299.
[85] N. V. Raghavan, R. E. Davis, *J. Cryst. Mol. Struct.* **1976**, *6*, 73.
[86] M. I. Bruce, N. N. Zaitseva, B. W. Skelton, N. Somers, A. H. White, *Aust. J. Chem.* **2003**, *56*, 509.
[87] I. Ara, J. R. Berenguer, E. Eguizábal, J. Forniés, E. Lalinde, A. Martín, *Eur. J. Inorg. Chem.* **2001**, 1631.

[88] S. Mihan, K. Sunkel, W. Beck, *Chem. Eur. J.* **1999**, *5*, 745.
[89] S. Tanaka, T. Yoshida, T. Adachi, T. Yoshida, K. Onitsuka, K. Sonogashira, *Chem. Lett.* **1994**, 877.
[90] G. A. Carriedo, D. Miguel, V. Riera, X. Solans, M. Font-Altaba, M. Coll, *J. Organomet. Chem.* **1986**, *299*, C43.
[91] G. A. Carriedo, D. Miguel, V. Riera, X. Solans, *J. Chem. Soc. Dalton Trans.* **1987**, 2867.
[92] H. V. R. Dias, H. V. K. Diyabalanage, C. S. P. Gamage, *Chem. Commun.* **2005**, 1619.
[93] S. S. Y. Chui, M. F. Y. Ng, C. M. Che, *Chem. Eur. J.* **2005**, *11*, 1739.
[94] Q. H. Wei, G. Q. Yin, Z. Ma, L. X. Shi, Z. N. Chen, *Chem. Commun.* **2003**, 2188.
[95] I. de los Rios, M. J. Tenorio, M. C. Puerta, P. Valerga, *Organometallics* **1998**, *17*, 3356.
[96] I. Ara, J. Forniés, J. Gómez, E. Lalinde, R. Merino, M. T. Moreno, *Inorg. Chem. Commun.* **1999**, *2*, 62.
[97] S. Yamazaki, A. J. Deeming, D. M. Speel, D. E. Hibbs, M. B. Hursthouse, K. M. A. Malik, *Chem. Commun.* **1997**, 177.
[98] P. Espinet, J. Forniés, F. Martínez, M. Sotés, E. Lalinde, M. T. Moreno, A. Ruiz, A. J. Welch, *J. Organomet. Chem.* **1991**, *403*, 253.
[99] J. Forniés, M. A. Gómez-Saso, F. Martínez, E. Lalinde, M. T. Moreno, A. J. Welch, *New J. Chem.* **1992**, *16*, 483.
[100] H. Lang, A. Kohler, L. Zsolnai, *Chem. Commun.* **1996**, 2043.
[101] K. Kohler, S. J. Silverio, I. Hyla-Kryspin, R. Gleiter, L. Zsolnai, A. Driess, G. Huttner, H. Lang, *Organometallics* **1997**, *16*, 4970.
[102] D. M. P. Mingos, J. Yan, S. Menzer, D. J. Williams, *Angew. Chem.* **1995**, *107*, 2045; *Angew. Chem. Int. Ed. Engl.* **1995**, *34*, 1894.
[103] S. K. Yip, E. C.-C. Cheng, L.-H. Yuan, N. Zhu, V. W. W. Yam, *Angew. Chem.* **2004**, *116*, 5062; *Angew. Chem. Int. Ed.* **2004**, *43*, 4954.
[104] P. Schulte, U. Behrens, *Chem. Commun.* **1998**, 1633.
[105] G. A. Ardizzoia, G. La Monica, A. Maspero, M. Moret, N. Masciocchi, *Inorg. Chem.* **1997**, *36*, 2321.
[106] D. Carmona, J. Ferrer, F. J. Lahoz, L. A. Oro, M. P. Lamata, *Organometallics* **1996**, *15*, 5175.
[107] A. A. Mohamed, L. M. Pérez, J. P. Fackler Jr., *Inorg. Chim. Acta* **2005**, *358*, 1657.
[108] A. A. Mohamed, A. Burini, J. P. Fackler Jr., *J. Am. Chem. Soc.* **2005**, *127*, 5012.
[109] G. A. Ardizzoia, G. La Monica, A. Maspero, N. Masciocchi, M. Moret, *Eur. J. Inorg. Chem.* **1999**, 1301.
[110] R. G. Raptis, H. H. Murray, J. P. Fackler Jr., *Chem. Commun.* **1987**, 737.
[111] G. Yang, R. G. Raptis, *Inorg. Chim. Acta* **2003**, *352*, 98.
[112] J. Forniés, A. Martín, V. Sicilia, P. Villarroya, *Organometallics* **2000**, *19*, 1107.
[113] J. Forniés, A. Martín, R. Navarro, V. Sicilia, P. Villarroya, A. G. Orpen, *J. Chem. Soc. Dalton Trans.* **1998**, 3721.
[114] L. R. Falvello, J. Forniés, A. Martín, R. Navarro, V. Sicilia, P. Villarroya, *Inorg. Chem.* **1997**, *36*, 6166.
[115] J. Forniés, A. Martín, R. Navarro, V. Sicilia, P. Villarroya, *Organometallics* **1996**, *15*, 1826.
[116] J. R. Berenguer, E. Eguizábal, L. R. Falvello, J. Forniés, E. Lalinde, A. Martín, *Organometallics* **2000**, *19*, 490.
[117] J. R. Berenguer, E. Eguizábal, L. R. Falvello, J. Forniés, E. Lalinde, A. Martín, *Organometallics* **1999**, *18*, 1653.
[118] I. Ara, L. R. Falvello, S. Fernandez, J. Forniés, E. Lalinde, A. Martín, M. T. Moreno, *Organometallics* **1997**, *16*, 5923.
[119] J. Forniés, E. Lalinde, A. Martín, M. T. Moreno, *J. Chem. Soc. Dalton Trans.* **1994**, 135.
[120] H. K. Yip, H. M. Lin, Y. Wang, C. M. Che, *J. Chem. Soc. Dalton Trans.* **1993**, 2939.
[121] L. Sacksteder, E. Baralt, B. A. Degraff, C. M. Lukehart, J. N. Demas, *Inorg. Chem.* **1991**, *30*, 2468.
[122] W. M. Kwok, D. L. Phillips, P. K. Y. Yeung, V. W. W. Yam, *J. Phys. Chem. A* **1997**, *101*, 9286.
[123] C. H. Tao, N. Zhu, V. W. W. Yam, *Chem. Eur. J.* **2005**, *11*, 1647.
[124] K. Onitsuka, M. Fujimoto, H. Kitajima, N. Ohshiro, F. Takei, S. Takahashi, *Chem. Eur. J.* **2004**, *10*, 6433.
[125] F. Zhuravlev, J. A. Gladysz, *Chem. Eur. J.* **2004**, *10*, 6510.
[126] L. A. Emmert, W. Choi, J. A. Marshall, J. Yang, L. A. Meyer, J. A. Brozik, *J. Phys. Chem. A* **2003**, *107*, 11340.
[127] J. Benito, J. R. Berenguer, J. Forniés, B. Gil, J. Gómez, E. Lalinde, *Dalton Trans.* **2003**, 4331.
[128] The HOMO is usually viewed as an antibonding combination of the highest occupied π orbital of the sp-carbon alkynyl fragments and the adequate filled d orbital of the platinum fragment.
[129] H. Masai, K. Sonogashira, H. Hagihara, *Bull. Chem. Soc. Jpn.* **1971**, *44*, 2226.
[130] C. Y. Wong, C. M. Che, M. C. W. Chan, J. Han, K. H. Leung, D. L. Phillips, K. Y. Wong, N. Zhu, *J. Am. Chem. Soc.* **2005**, *127*, 13997.
[131] V. W. W. Yam, K.-L. Yu, K. M. C. Wong, K. K. Cheung, *Organometallics* **2001**, *20*, 721.
[132] V. W. W. Yam, K. L. Cheung, E. C. C. Cheng, N. Zhu, K. K. Cheung, *Dalton Trans.* **2003**, 1830.
[133] Q. S. Li, F. B. Xu, D. J. Cui, K. Yu, X. S. Zheng, X. B. Leng, H. B. Song, *Dalton Trans.* **2003**, 1551.
[134] Y. Y. Liu, S. W. Lai, C. M. Che, K. K. Cheung, Z. Y. Zhou, *Organometallics* **2002**, *21*, 2275.
[135] Q. H. Wei, G. Q. Yin, L. Y. Zhang, L. X. Shi, Z. W. Mao, Z. N. Cheng, *Inorg. Chem.* **2004**, *43*, 3484.
[136] V. W. W. Yam, C. K. Hui, S. Y. Yu, N. Zhu, *Inorg. Chem.* **2004**, *43*, 812, and references therein.
[137] A. Vogler, H. Kunkely, *J. Am. Chem. Soc.* **1986**, *108*, 7211.
[138] K. R. Kyle, C. K. Ryu, J. A. Dibenedetto, P. C. Ford, *J. Am. Chem. Soc.* **1991**, *113*, 2954.
[139] P. C. Ford, E. Cariati, J. Bourassa, *Chem. Rev.* **1999**, *99*, 3625.
[140] V. W. W. Yam, E. C. C. Cheng, N. Zhu, *Angew. Chem.* **2001**, *113*, 1813; *Angew. Chem. Int. Ed.* **2001**, *40*, 1763.
[141] I. Ara, J. R. Berenguer, E. Eguizábal, J. Forniés, J. Gómez, E. Lalinde, *J. Organomet. Chem.* **2003**, *670*, 221.
[142] L. Hao, M. A. Mansour, R. J. Lachicotte, H. J. Gysling, R. Eisenberg, *Inorg. Chem.* **2000**, *39*, 5520.
[143] J. Forniés, J. Gómez, E. Lalinde, M. T. Moreno, *Inorg. Chim. Acta* **2003**, *347*, 145.
[144] V. W. W. Yam, K. L. Yu, K. K. Cheung, *J. Chem. Soc. Dalton Trans.* **1999**, 2913.
[145] J. N. G. Demas, A. Crosby, *J. Phys. Chem.* **1971**, *75*, 991.
[146] G. J. Kubas, *Inorg. Synth.* **1990**, *19*, 90.
[147] J. Vicente, M. T. Chicote, *Inorg. Synth.* **1998**, *32*, 175.
[148] W. A. Herrmann, C. Brossmer, K. Ofele, C. P. Reisinger, T. Priermeier, M. Beller, H. Fischer, *Angew. Chem.* **1995**, *107*, 1989; *Angew. Chem. Int. Ed. Engl.* **1995**, *34*, 1844.
[149] SAINT integration software, Bruker Analytical X-ray Systems, Madison, WI, **1994**.
[150] CrysAlis RED, CCD Camera Data Reduction Program, Oxford Diffraction, Oxford, UK, **2004**.
[151] G. M. Sheldrick, SADABS Empirical Absorption Correction Program, University of Göttingen, Göttingen (Germany), **1996**.
[152] G. M. Sheldrick, SHELXL-97, A Program for Crystal Structure Determination, University of Göttingen, Göttingen (Germany), **1997**.

Received: February 1, 2006
Published online: July 18, 2006

